Control Theory MA3005
Part II : Controller design

Quang-Cuong Pham
School of Mechanical and Aerospace Engineering
Nanyang Technological University, Singapore

March 25, 2017

Disclaimer These notes are provided to help the students of MA3005 get a more systematic understanding of the topics presented during the lecture. I assume no liability or responsibility for any errors or omissions in the content. Students are advised to refer to the live lecture and lecture slides for exam-related matters.

Contents

0 Recapitulation of part I **4**
- 0.1 Stability and transient behavior . . . 4
  - 0.1.1 Characteristic equation and stability . . . 4
  - 0.1.2 Transient behavior . . . 6
- 0.2 Steady-state error . . . 7
  - 0.2.1 Definition . . . 7
  - 0.2.2 System type and steady-state error . . . 8

1 Introduction to controller design **11**
- 1.1 A simple controller design problem . . . 11
  - 1.1.1 Problem setting . . . 11
  - 1.1.2 First attempt : proportional control . . . 12
  - 1.1.3 Second attempt : proportional-derivative control . . . 13
  - 1.1.4 Third attempt : PD control with lag compensation . . . 15
  - 1.1.5 Summary . . . 16
- 1.2 Effects of basic control actions on system performance . . . 16
  - 1.2.1 Effects of derivative action . . . 16
  - 1.2.2 Effects of integral action . . . 17
  - 1.2.3 Summary . . . 18

2 Controller design by the root locus method **19**
- 2.1 Introduction to root locus . . . 19
  - 2.1.1 Definition of root locus . . . 19
  - 2.1.2 Root locus of the simple helicopter system with PD control . . . 20
  - 2.1.3 Characteristic equations (CE) of feedback systems with variable gains . . . 21
- 2.2 Steps to sketch the root locus . . . 23
  - 2.2.1 Poles, zeros, branches . . . 23
  - 2.2.2 Infinite branches, asymptotes . . . 24
  - 2.2.3 Poles/zeros on the real axis . . . 25
  - 2.2.4 Departure/arrival angles from/to complex poles/zeros 26
  - 2.2.5 Break-in/break-out points . . . 28

2.2.6 Crossing of imaginary axis 29
2.2.7 Summary 30
2.3 Transient response design by gain adjustment 31
2.4 Improving transient behavior by lead compensation 33
2.4.1 PD controller 33
2.4.2 Lead compensator 36
2.5 Reducing steady-state error by lag compensation 41
2.5.1 PI controller 41
2.5.2 Lag compensator 45
2.6 Improving transient behavior *and* reducing steady-state error 47
2.6.1 PID controller 48
2.6.2 Lead-lag compensator 48
2.7 Physical implementation of compensators 48
2.7.1 Lead compensators 48
2.7.2 Lag compensators 49
2.8 Parallel compensation 50
2.9 Summary 51

3 Controller design by the frequency response method 52
3.1 Introduction to frequency response 52
3.2 Bode plots : generalities 55
3.2.1 Interpretation of Bode plots 55
3.2.2 Filters 57
3.3 Bode plots : sketching 59
3.3.1 Properties 59
3.3.2 Bode plots of basic functions 60
3.3.3 Bode plots of complex functions 65
3.4 Bode plots : analysis 69
3.4.1 Determining system type and system order 70
3.4.2 Determining position and velocity constants and steady-state errors 70
3.4.3 Stability margins 73
3.4.4 Some remarks on controller design by the frequency-response method 78

Chapter 0

Recapitulation of part I

0.1 Stability and transient behavior

0.1.1 Characteristic equation and stability

The stability of a system is determined by the *denominator* of the transfer function, which is also called the *Characteristic Equation* (CE). More precisely, it is determined by the locations of the roots of the CE – also called *poles* – in the complex plane.

- If all the poles are in the open left half-plane, the system is *stable*, see Fig. 0.1;
- If all the poles are in the closed left half-plane, and a pair of roots are on the imaginary axis, the system is *marginally stable*, see Fig. 0.2;
- If at least one pole is in the open right half-plane, the system is *unstable*, see Fig. 0.3.

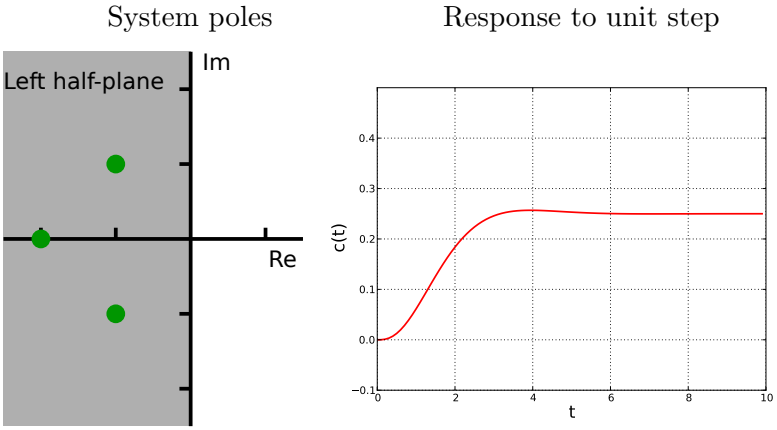

Figure 0.1: A stable system with transfer function $\frac{C}{R} = \frac{1}{s^3+4s^2+6s+4}$. The CE is $s^3 + 4s^2 + 6s + 4$, which has three roots: $-1 \pm j, -2$.

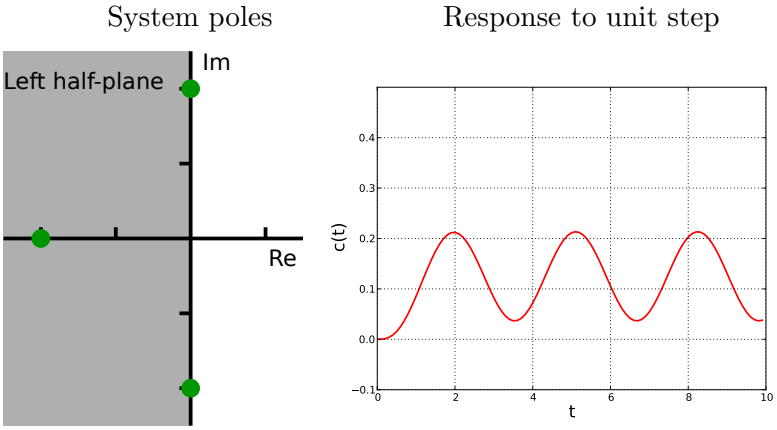

Figure 0.2: A marginally stable system with transfer function $\frac{C}{R} = \frac{1}{s^3+2s^2+4s+8}$. The CE is $s^3 + 2s^2 + 4s + 8$, which has three roots: $\pm 2j, -2$. The frequency of oscillation is given by ω, where ω is the norm of the roots on the imaginary axis (here $\omega = 2\,\mathrm{rad/s}$).

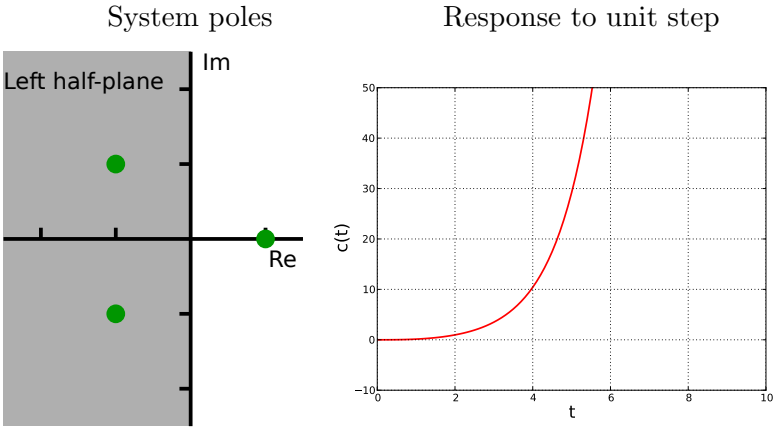

Figure 0.3: An unstable system with transfer function $\frac{C}{R} = \frac{1}{s^3+s^2-2}$. The CE is $s^3 + s^2 - 2$, which has three roots: $-1 \pm j, 1$.

0.1.2 Transient behavior

Once a system has been determined as stable, one can investigate its transient behavior, roughly, how fast does the system response converge to its final value. This is measured by quantities such as settling time or maximum overshoot.

The transient behavior depends primarily on the precise location of the dominant (i.e. rightmost) poles in the complex plane. The further the dominant poles to the left, the faster the convergence (the smaller the settling time and the maximum overshoot). Compare Fig. 0.4, red line and Fig. 0.4, green line : both systems are stable, but the red system converges faster than the green system, since its dominant poles are located more to the left ($-2 \pm j$ vs $-1 \pm j$).

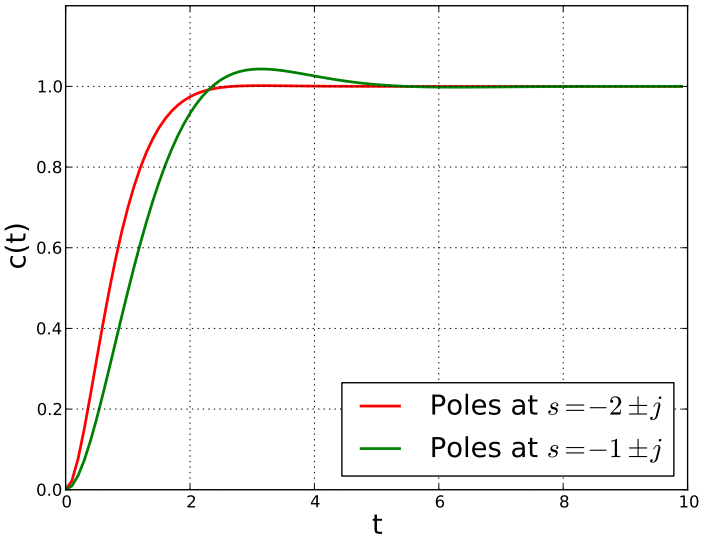

Figure 0.4: Comparison of the convergence speed of two systems. Red: unit-step response of a system with transfer function $\frac{C}{R} = \frac{5}{s^2+4s+5}$. The CE is $s^2 + 4s + 5$, which has two roots: $-2 \pm j$. Green: unit-step response of a system with transfer function $\frac{C}{R} = \frac{2}{s^2+2s+2}$. The CE is $s^2 + 2s + 2$, which has two roots: $-1 \pm j$.

The transient behavior (in particular, whether the system oscillates, etc.) is also affected by other quantities such as the damping ratio ζ and the undamped natural frequency ω_0. For more details, refer to the slides from Part I of the course.

0.2 Steady-state error

0.2.1 Definition

Consider a feedback system as in Fig. 0.5.

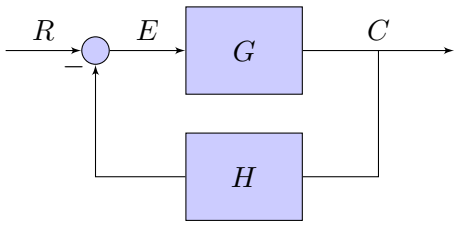

Figure 0.5: Error signal: $E = R - C$

The steady-state error (if it exists) is defined by

$$e_{\text{ss}} := \lim_{t\to\infty} e(t). \tag{1}$$

If the system is stable, one can apply the Finaly Value Theorem to obtain

$$\lim_{t\to\infty} e(t) = \lim_{s\to 0} sE(s).$$

In general, one would like the steady-state error to be as small as possible, ideally zero.

0.2.2 System type and steady-state error

In general, to calculate the steady-state error, one uses the FVT as in equation (1). However, if the system is stable and *unity-feedback*, then one can determine the system type and use this information to obtain the steady-state error much more easily.

Let G be the feedforward transfer function. Assume that G is written as

$$G = \frac{N(s)}{s^k D(s)},$$

where N and D are not factorizable by s. Then the type of the system is given by the integer k. Fig. 0.6 shows the general form of systems of types 1, 2 and 3.

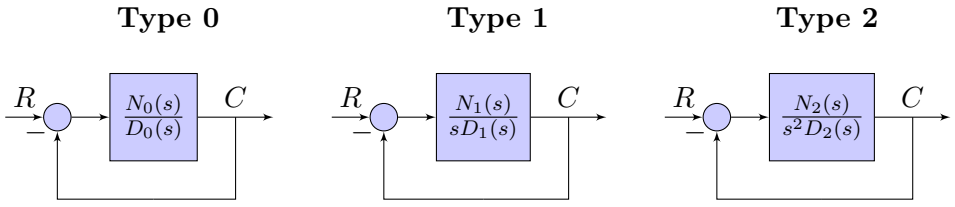

Figure 0.6: Systems of types 0, 1 and 2. Note that $N_0, N_1, N_2, D_0, D_1, D_2$ should not be factorizable by s.

Let us carry further the computation of the steady-state error for a stable unity-feedback system.

$$sE(s) = s(R(s) - C(s)) = s\left(R(s) - \frac{G(s)}{1+G(s)}R(s)\right) = \frac{s}{1+G(s)}R(s).$$

For unit-step input, one has $R(s) = 1/s$. Thus,

$$sE(s) = \frac{s}{1+G(s)} * \frac{1}{s} = \frac{1}{1+G(s)} \xrightarrow[s\to 0]{} \frac{1}{1+\lim_{s\to 0} G(s)}.$$

For a system of type 0, one has

$$\lim_{s\to 0} G(s) = \lim_{s\to 0} \frac{N_0(s)}{D_0(s)} = \frac{N_0(0)}{D_0(0)}.$$

Thus, the steady-state error of a system of type 0 for unit-step input is given by

$$e_{\rm ss} = \frac{1}{1+\frac{N_0(0)}{D_0(0)}}.$$

Carrying out similar calculations, one obtains the following table, which shows the steady-state errors of systems of types 0, 1, 2, 3 for unit-step, unit-ramp and unit-parabola inputs.

System type	Step input	Ramp input	Parabolic input
Type 0	$\frac{1}{1+K_p}$	∞	∞
Type 1	0	$\frac{1}{K_v}$	∞
Type 2	0	0	$\frac{1}{K_a}$
Type 3	0	0	0

Table 1: Steady-state errors of systems of different types and for different inputs.

The constants K_p, K_v, and K_a are defined as below

- for a system of type 0, $K_p := \frac{N_0(0)}{D_0(0)}$ (position constant);
- for a system of type 1, $K_v := \frac{N_1(0)}{D_1(0)}$ (velocity constant);
- for a system of type 2, $K_a := \frac{N_2(0)}{D_2(0)}$ (acceleration constant).

Example 1. Consider a unity-feedback system with feedforward transfer function

$$G(s) = \frac{s^2+2s}{2s^4+s^3+3s^2}.$$

What is the steady-state error of the system for unit-ramp and unit-parabola inputs?

Answer: One can simplify G as follows

$$G(s) = \frac{s(s+2)}{s^2(2s^2+s+3)} = \frac{s+2}{s(2s^2+s+3)},$$

which implies that the system is of type 1, with

$$N(s) = s+2 \quad ; \quad D(s) = 2s^2+s+3.$$

From the table, the steady-state error for unit-ramp input is given by

$$e_{\text{ss}} = \frac{1}{K_v},$$

where the velocity constant K_v is given by

$$K_v = \frac{N(0)}{D(0)} = \frac{2}{3}.$$

Thus $e_{\text{ss}} = 1.5$.

Also from the table, the steady-state error for unit-parabola input is ∞.

Chapter 1

Introduction to controller design

1.1 A simple controller design problem

1.1.1 Problem setting

Consider the helicopter in Fig. 1.1. Applying Newton's second law in the vertical axis, we obtain

$$m\ddot{z} = F_{\text{lift}} - mg, \tag{1.1}$$

where $g = 9.81\,\text{m}\cdot\text{s}^{-1}$ is the gravitational coefficient.

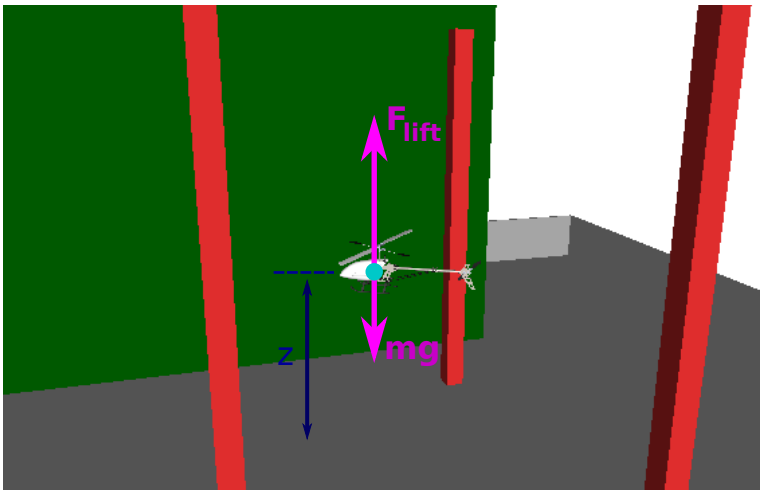

Figure 1.1: A helicopter.

The lift force F_{lift} is proportional to the rotor speed ω_{rotor}, which is in turn proportional to the electric current i_{rotor} fed into the motor. One can

thus write

$$F_{\text{lift}} = k i_{\text{rotor}},$$

where k is a positive constant.

To eliminate the constant term mg, let us note $i = i_{\text{rotor}} - \frac{mg}{k}$. Equation (1.1) becomes

$$m\ddot{z} = F_{\text{lift}} - mg = k i_{\text{rotor}} - mg = ki. \tag{1.2}$$

Taking the Laplace transform of the above equation, we have

$$ms^2 Z = kI, \quad \text{i.e. } Z = \frac{k}{ms^2} I,$$

which corresponds to the following block diagram

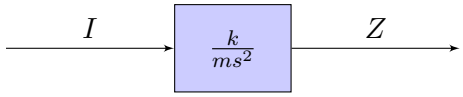

Figure 1.2: Block diagram of the quadcopter.

Assume that we want the altitude z of the quadcopter (the output) to follow – or *track* – a desired profile z_{ref}, which can be for instance a constant altitude (step input), or a linearly increasing altitude (ramp input), etc. The control problem we have is : how to regulate the electric current i_{rotor} (or i) so that z follows as closely as possible z_{ref}?

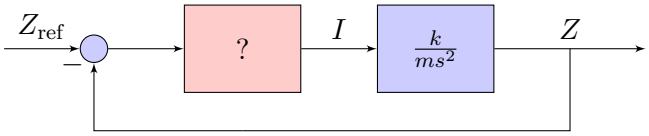

Figure 1.3: Control problem.

1.1.2 First attempt : proportional control

Consider now the following *control law*, also known as *proportional control*

$$i = K(z_{\text{ref}} - z),$$

where K is a positive and constant *proportional gain* that we can choose. Note that we have a feedback system, in the sense that the output Z is fed back into the definition of the control. Note also that the measure of the output z is assumed to be perfect.

In the Laplace domain, we have

$$I = K\left(Z_{\text{ref}} - Z\right),$$

which leads to the following block diagram

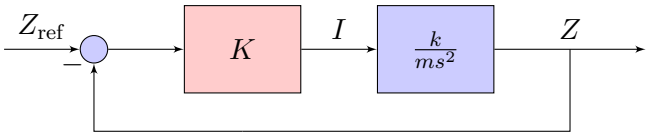

Figure 1.4: Proportional control.

The transfer function of this system can be calculated as

$$\frac{Z}{Z_{\text{ref}}} = \frac{Kk}{ms^2 + Kk}.$$

Since Kk is positive, there are two complex poles $\pm j\sqrt{Kk/m}$. Thus, this system is *unstable* for all values of the gain K. Actually, it oscillates with frequency $\omega = \sqrt{Kk/m}$, see Fig. 1.5.

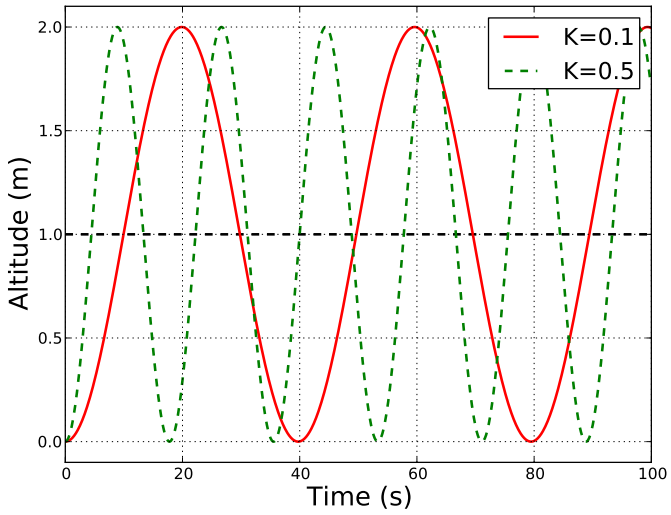

Figure 1.5: Step response of the helicopter system ($m = 2$ and $k = 0.5$) with with proportional control.

From this analysis, it is clear that a proportional controller is insufficient to achieve the goal of tracking closely a given input.

1.1.3 Second attempt : proportional-derivative control

Consider now another control law, also known as *proportional-derivative control*

$$i = K_D(\dot{z}_{\text{ref}} - \dot{z}) + K_P\,(z_{\text{ref}} - z)\,.$$

Note that we assume here that not only the current altitude z of the quadcopter can be measured, but also the derivative of the altitude $\dot{z}$.

Here we have two control gains that we can choose, namely K_P (the proportional gain) and K_D (the derivative gain).

In the Laplace domain, we have

$$I = K_D(sZ_{\text{ref}} - sZ) + K_P(Z_{\text{ref}} - Z) = (K_D s + K_P)(Z_{\text{ref}} - Z),$$

which leads to the following block diagram.

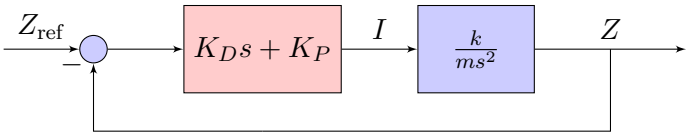

Figure 1.6: Proportional-derivative control.

The transfer function of this system can be calculated as

$$\frac{Z}{Z_{\text{ref}}} = \frac{K_D k s + K_P k}{ms^2 + K_D k s + K_P k}.$$

Fig. 1.7 shows the response of the system to a step input for various values of K_D and K_P.

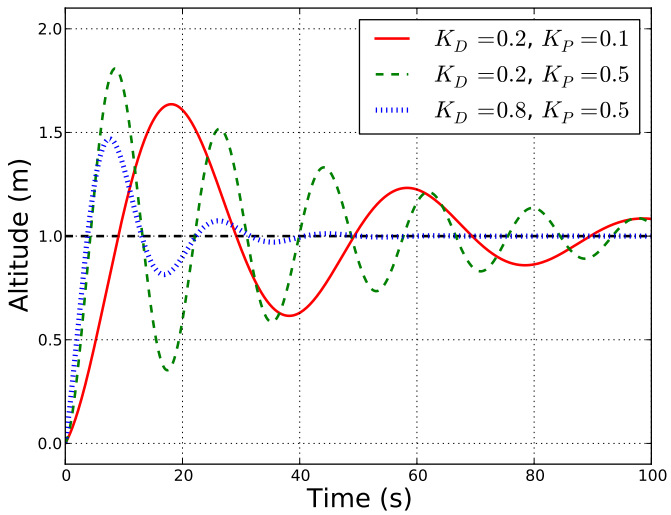

Figure 1.7: Step response of the helicopter system ($m = 2$ and $k = 0.5$) with proportional-derivative control.

Note that the tracking error for step input goes to 0 for all the PD controllers. But what happens for other types of inputs? Assume for instance

that we want the helicopter to ascend very quickly, namely, to follow the unit *parabolic input*

$$z_{\text{ref}} = t^2, \quad Z_{\text{ref}} = \frac{2}{s^3}.$$

Fig. 1.8 shows the *tracking error* of the system to the unit parabolic input

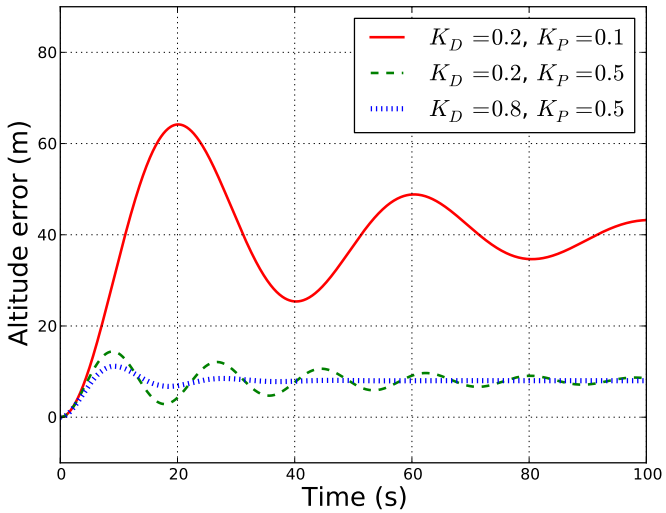

Figure 1.8: Tracking error of the system with proportional-derivative control subject to the unit parabolic input

Clearly, the tracking error for the unit parabolic input does not converge to zero for any gain. It may be possible to make this error smaller by increasing the gains, but then the system will be more sensitive to noise.

1.1.4 Third attempt : PD control with lag compensation

To decrease the tracking error for the unit parabolic input, let us consider the following *lag compensator*, which is cascaded in series with the PD controller

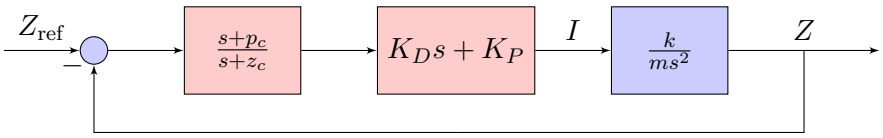

Figure 1.9: Lag compensation in series with PD control.

This compensated system has a much lower steady-state tracking error for the parabolic input (Fig. 1.10A) while keeping almost the same transient behavior as the uncompensated system (Fig. 1.10B).

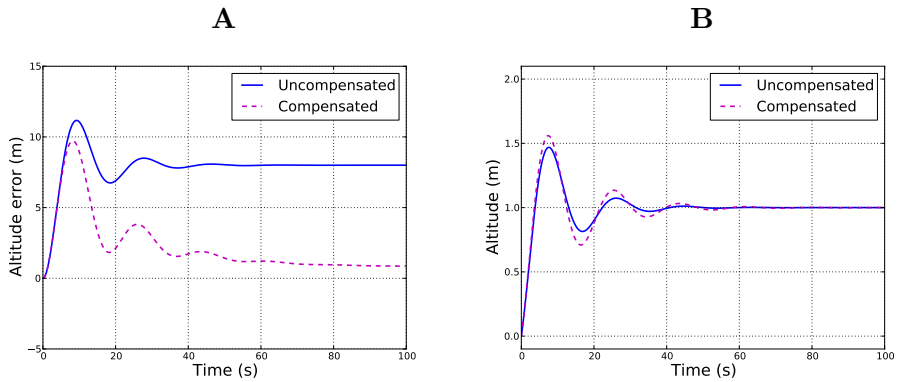

Figure 1.10: System with proportional-derivative control and without/with lag compensation ($m = 2$, $k = 0.5$, $K_D = 0.8$, $K_P = 0.5$, $p_c = 0.05$, $z_c = 0.005$). **A**: Tracking error to unit parabolic input. **B**: System response to unit step input.

1.1.5 Summary

Summary 1. The objective of controller design is to increase the performance of a given *unalterable system* by connecting it to various types of controllers. The performance of a controlled system is measured by

- its *transient behavior* (stability, tracking speed, etc.);
- its *steady-state errors* for various types of inputs (step, ramp, parabolic, etc.)

In Chapter 2, we shall study the *root locus* method, which is used for time domain controller design.

In Chapter 3, we shall study the *frequency response* method, which is used for frequency domain controller design.

1.2 Effects of basic control actions on system performance

Let us examine how basic control actions, such as derivative and integral actions, influence system performance.

1.2.1 Effects of derivative action

Derivative action means that we introduce a Ks term in the feedforward path. Note that pure derivative controllers are seldom used: in practice, we always have proportional-derivative control. The general form of a PD-controlled system is

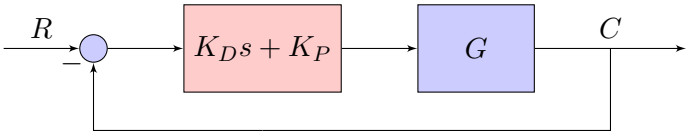

Figure 1.11: Proportional-derivative controller.

We have seen in the example of the helicopter system (Section 1.1.3) that the introduction of the derivative action helps *stabilize* an otherwise unstable system. Intuitively, the derivative action responds to the *rate of change of the error*, thus it can produce a significant correction before the magnitude of the error becomes too large.

Mathematically, the derivative action adds damping – therefore stability – to the system. Consider again the helicopter system, whose characteristic equation is

- $ms^2 + K_P k$ (P control) or
- $ms^2 + K_D k s + K_P k$ (PD control).

The damping coefficient is $\zeta = 0$ in P-control and $\zeta = \frac{K_D k}{2\sqrt{m K_P k}}$ in PD control. The larger K_D, the larger ζ.

1.2.2 Effects of integral action

The main effect of integral action is to *eliminate the steady-state error*. Consider a first-order system with a proportional control as below

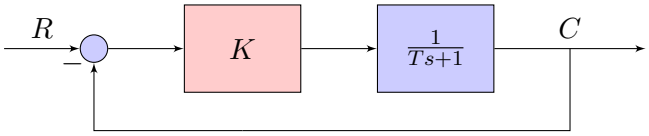

Figure 1.12: First order system with proportional controller.

The controlled system is of type 0, therefore, the steady-state error for unit-step input is

$$\lim_{t\to\infty} e(t) = \frac{1}{1+K}.$$

Thus, no matter the value of K, we shall always have a non-zero steady-state error for unit-step input (offset). This error can go to zero if the gain K is chosen very large, but in this case, the system will also become more sensitive to noise.

Consider now the same system but with integral control

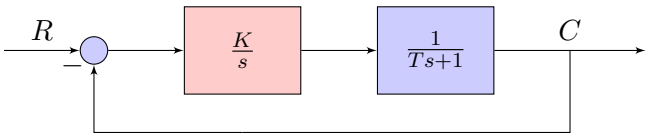

Figure 1.13: First order system with integral controller.

The controlled system is now of type 1, therefore, the steady-state error for unit-step input is 0 for any gain K, i.e.

$$\lim_{t\to\infty} e(t) = 0.$$

The side-effect of integral controllers is that they tend to make the system less stable.

1.2.3 Summary

Summary 2. The main effects of basic control actions are:

- Derivative action can improve the *transient behavior* by making the system more stable and/or respond faster;
- Integral action can reduce or elimininate *steady-state errors*. However, it also tends to make the system less stable.

Designing controllers thus consists in dosing the appropriate amounts of proportional/derivative/integral/etc. actions so as to achieve the control objectives in terms of both transient behavior and steady-state errors (cf. Summary 1).

Chapter 2

Controller design by the root locus method

2.1 Introduction to root locus

2.1.1 Definition of root locus

Consider a polynomial P in one complex variable $s \in \mathbb{C}$ and parameterized by a positive parameter $K \geq 0$, that is

$$\begin{aligned} P: \quad \mathbb{C} &\to \mathbb{C} \\ s &\mapsto P(K, s). \end{aligned}$$

For each value of K, the polynomial $P(K, s)$ will have n roots, where n is the degree of P. The locus of these n roots when K varies is called the *root locus* of P.

Example 2. Consider the polynomial

$$P(K, s) = s^2 + (2 + K)s + 5.$$

P has degree two. Thus, for each value of K, P will have two (complex) roots.

- When $K = 0$, $P(K, s) = s^2 + 2s + 5$. The discriminant is $\Delta = 2^2 - 4 * 5 = -16$, thus P has two complex roots at $-1 \pm 2j$;
- When $K = 1$, $P(K, s) = s^2 + 3s + 5$. The discriminant is $\Delta = 3^2 - 4 * 5 = -11$, thus P has two complex roots at $\frac{-3 \pm j\sqrt{11}}{2}$, i.e. $-1.5 \pm 1.7j$;
- When $K = 2$, $P(K, s) = s^2 + 7s + 5$. The discriminant is $\Delta = 7^2 - 4 * 5 = 29$, thus P has two real roots at $\frac{-7 \pm j\sqrt{29}}{2}$, i.e. -6.2 and -0.8;

- etc.

Fig. 2.1 shows the locations of the roots for K varying between 0 and 10 as well as for the specific values $K = 0, 1, 5$ just discussed.

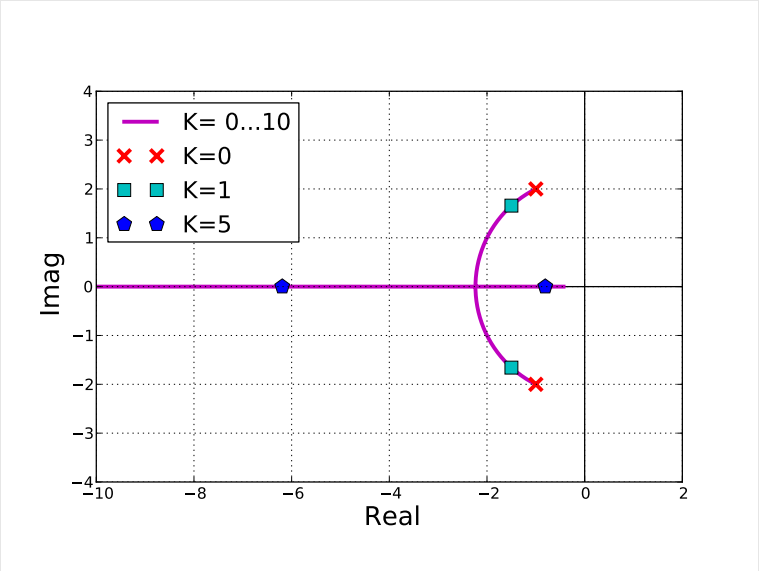

Figure 2.1: Root locus of $P(K, s) = s^2 + (2 + K)s + 5$ in the complex plane.

2.1.2 Root locus of the simple helicopter system with PD control

Consider the helicopter system with PD control discussed in Section 1.1.3. Recall that its transfer function is

$$\frac{Z}{Z_{\text{ref}}} = \frac{K_D k s + K_P k}{m s^2 + K_D k s + K_P k}.$$

Assume that the proportional and the derivative gains K_D, K_P cannot be set independently, but are instead equal to a value: $K_D = K_P = K$. The transfer function becomes

$$\frac{Z}{Z_{\text{ref}}} = \frac{K k (s + 1)}{m s^2 + K k s + K k}.$$

The root locus of

$$P(K, s) = m s^2 + K k s + K k \tag{2.1}$$

can be plotted as in Fig. 2.2.

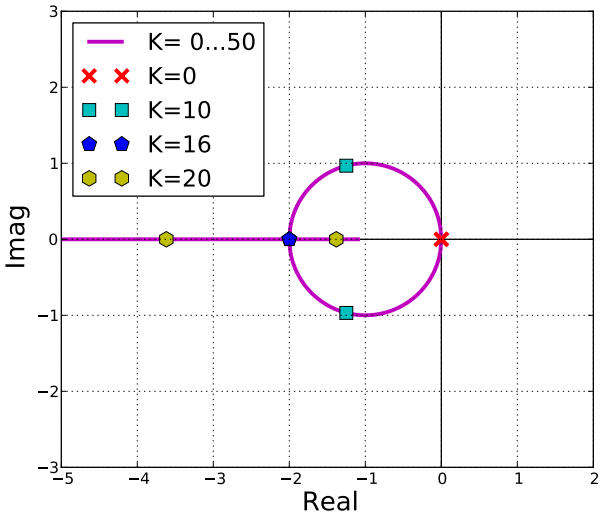

Figure 2.2: Root locus of the helicopter system with PD control. The characteristic polynomial is $P(K, s) = ms^2 + Kks + Kk$, with $m = 2$ and $k = 0.5$.

From the root locus, we can obtain the following information

- The system is unstable for $K = 0$ (no control), but will be stable for all values $K > 0$.
- The system is underdamped $0 < K < 16$.
- The system is critically damped for $K = 16$.
- The system is overdamped for $K > 16$.

This information enables us to select the appropriate gain K to achieve given performance specifications in terms of transient behavior.

2.1.3 Characteristic equations (CE) of feedback systems with variable gains

Most systems we shall consider can be put in the form depicted in Fig. 2.3, where G and H are two *rational fractions* (i.e. fractions of polynomials) and K is a positive variable gain.

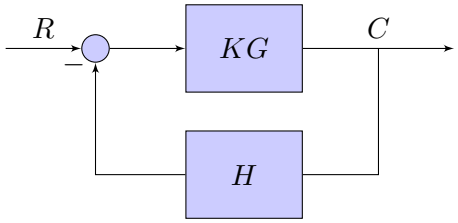

Figure 2.3: Typical feedback system with variable gain.

Assume G and H are of the form $\frac{N_G(s)}{D_G(s)}$, $\frac{N_H(s)}{D_H(s)}$, where N_G, D_G, N_H, D_H are polynomials in the variable s. The transfer function of the system is then

$$\frac{C}{R} = \frac{KG}{1+KGH} = \frac{\frac{KN_G}{D_G}}{1+\frac{KN_GN_H}{D_GD_H}} = \frac{KN_GD_H}{KN_GN_H+D_GD_H}. \tag{2.2}$$

Thus, the characteristic equation of the system is

$$KN_G(s)N_H(s) + D_G(s)D_H(s) = 0,$$

which can also be written

$$KN(s) + D(s) = 0,$$

where $N(s) = N_G(s)N_H(s)$ and $D(s) = D_G(s)D_H(s)$ are two polynomials in s.

Example 3. Consider the system

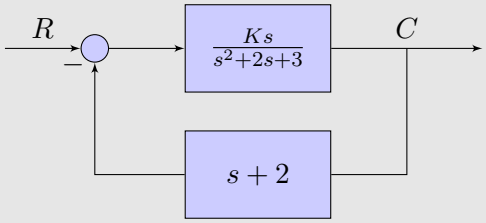

We have

- $N_G(s) = s$;
- $D_G(s) = s^2 + 2s + 3$;
- $N_H(s) = s + 2$;
- $D_H(s) = 1$.

Thus, the characteristic equation is

$$Ks(s+2) + (s^2 + 2s + 3) = 0,$$

which can also be rewritten as

$$K = -\frac{s^2 + 2s + 3}{s(s+2)}.$$

2.2 Steps to sketch the root locus

So how can we plot the root locus of a given system? We can use Matlab or Python. Here, we show how to sketch rapidly the root locus without using computers.

2.2.1 Poles, zeros, branches

Consider the characteristic equation (CE) in the general form

$$KN(s) + D(s) = 0.$$

The roots of $D(s)$ are called *poles* of the CE and the roots of $N(s)$ are called *zeros* of the CE.

- When $K = 0$, the CE becomes $D(s) = 0$. Thus, the poles of a CE are solutions of the CE when $K = 0$.
- When $K \to \infty$, $D(s)$ is negligible compared to $KN(s)$, thus the CE becomes $KN(s) = 0$. Therefore, the zeros of a CE are solutions of the CE when $K \to \infty$.

From the above, we can see that, when K varies from 0 to ∞, the root locus of the CE will describe in the complex plane a number of curves, which *depart from the poles* and *arrive at the zeros*. These curves are called the *branches* of the CE.

Example 4. Consider the CE

$$K(s^2 + 2s + 5) + (s^2 + 3s + 20) = 0.$$

The roots of $N(s)$ are $-1 \pm 2j$ and the roots of $D(s)$ are $-1.5 \pm 4.2j$. There are thus two branches, departing from $-1.5 \pm 4.2j$ and arriving at $-1 \pm 2j$, see Fig. 2.4.

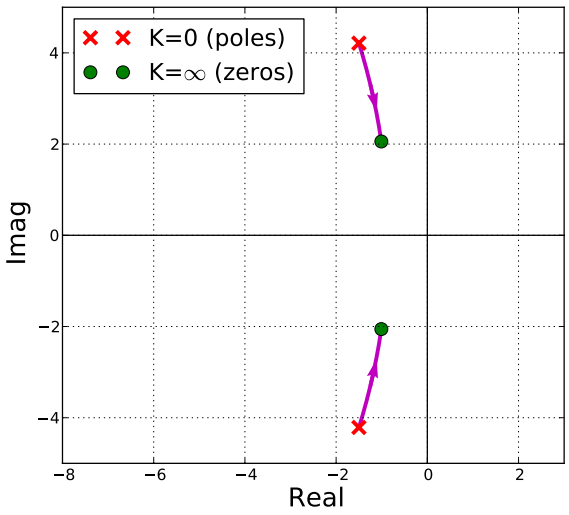

Figure 2.4: Root locus of $K(s^2+2s+5)+(s^2+3s+20)=0$, which has two finite branches.

2.2.2 Infinite branches, asymptotes

When there are more poles than zeros, some branches must arrive "at infinity" : we are then in the presence of *infinite branches*. The number of infinite branches is given by

$$n_{\text{infinite branches}} = n_{\text{poles}} - n_{\text{zeros}}.$$

Each infinite branch will "converge" to an asymptote, thus the number of asymptotes is $n_{\text{infinite branches}}$. The possible configurations of the asymptotes are given in Fig. 2.5.

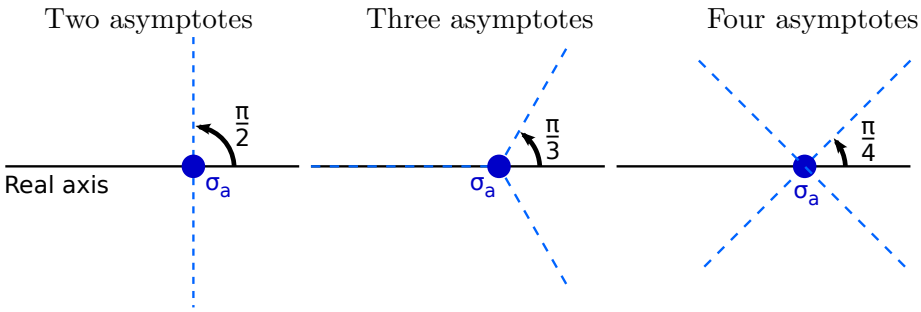

Figure 2.5: The configuration of the asymptotes is always fixed given the number N of asymptotes. Basically, the N asympotes divide the complex plane into N equal regions, and the angle from the real axis to the first asymptote is $\frac{\pi}{N}$.

Next, the intersection point of the asymptotes is given by

$$\sigma_a = \frac{\sum \text{poles} - \sum \text{zeros}}{n_{\text{poles}} - n_{\text{zeros}}}.$$

Example 5. Consider the CE

$$K(s + 0.5) + (s^2 + 2s + 5)(s^2 + 3s + 20) = 0.$$

There are four poles $(-1 \pm 2j, -1.5 \pm 4.2j)$ and one zero (-0.5), therefore $4 - 1 = 3$ infinite branches. The asymptotes meet at

$$\sigma_a = \frac{+0.5 - 1 - 1 - 1.5 - 1.5}{3} = -1.5.$$

See Fig. 2.6.

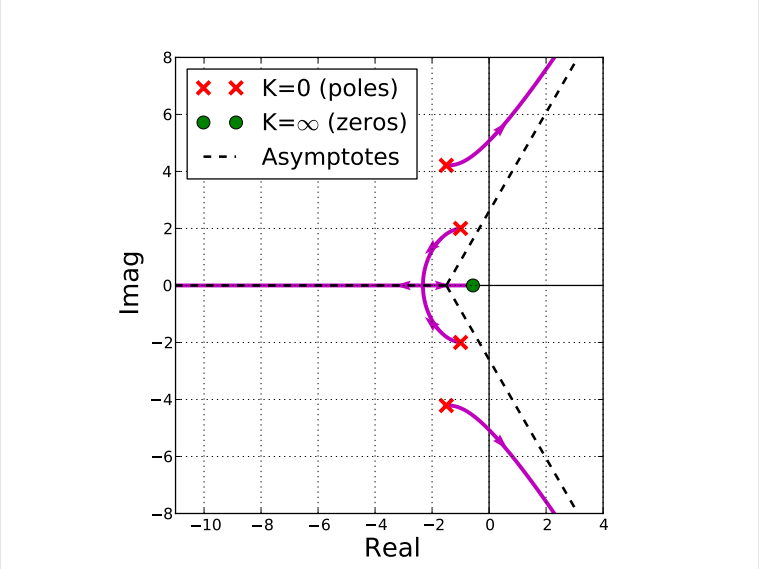

Figure 2.6: Root locus of $K(s + 0.5) + (s + 2s + 5)(s^2 + 3s + 20) = 0$, which has 1 finite and 3 infinite branches.

2.2.3 Poles/zeros on the real axis

When there are poles/zeros on the real axis, then parts of the root locus will be on the real axis. The rule is

> "Every point of the real axis that is on the left of an odd number of poles/zeros belongs to the root locus."

From this rule, one can determine entirely the root locus on the real axis, as well as the departure/arrival angles from/to the poles/zeros on the real axis.

Example 6. Fig. 2.7 and 2.8 depict two typical configurations of poles/zeros on the real axis and how we can determine the root locus as well as departure/arrival angles on the real axis.

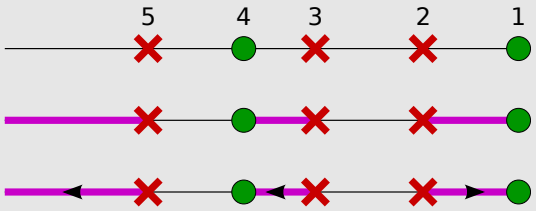

Figure 2.7: A configuration of poles/zeros on the real axis. Red disks denote the poles and green squares the zeros. Step 1: we number the poles/zeros starting with 1 on the right. Step 2: we highlight the spaces between points 1 and 2, between points 3 and 4, etc. as root locus. Step 3: we indicate the departure/arrival arrows (arrows must leave poles and arrive at zeros).

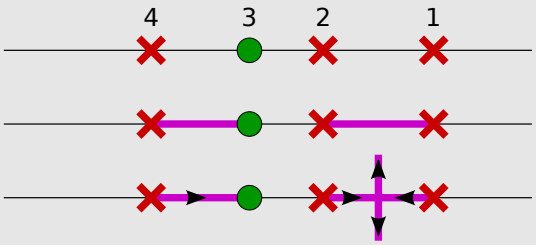

Figure 2.8: Another configuration. This configuration is the same as in Fig. 2.7, except that we have removed the rightmost zero. Doing so completely changes the root locus on the real axis. Note that, when determining the departure/arrival arrows, we have two arrows pointing towards each other between point 1 and point 2. This implies that there must exist a *break-out* between point 1 and point 2. Similarly, in case we have two arrows pointing *away* from each other, this will imply the existence of a *break-in* point.

2.2.4 Departure/arrival angles from/to complex poles/zeros

It is important to determine the departure/arrival angles from poles/zeros in order to have an accurate drawing of the root locus.

The angle of departure from a complex pole p is given by

$$\alpha_{\text{dep}}(p) = \pi - \sum_{\text{poles } p_i} \alpha_{p_i \to p} + \sum_{\text{zeros } z_i} \alpha_{z_i \to p}.$$

The angle $\alpha_{p_i \to p}$ can either be determined graphically, or computed as $\angle(p - p_i)$.

Note that, the angle of a complex number given in Cartesian form $x + yj$ is *not always* $\tan^{-1}(y/x)$! On modern calculators or in Matlab/Python, it can be obtained as

$$\angle(x + yj) = \text{arctan2}(y, x).$$

The angle of arrival to a complex pole z is given by

$$\alpha_{\text{arr}}(z) = \pi + \sum_{\text{poles } p_i} \alpha_{p_i \to z} - \sum_{\text{zeros } z_i} \alpha_{z_i \to z}.$$

Example 7. Consider again the CE

$$K(s + 0.5) + (s^2 + 2s + 5)(s^2 + 3s + 20) = 0.$$

We have seen in Example 5 that this CE has four poles (let us number them from highest to lowers: $p_1 = -1.5 + 4.2j$, $p_2 = -1 + 2j$, $p_3 = -1 - 2j$, $p_4 = -1.5 - 4.2j$) and one zero ($z = -0.5$). Let us calculate the departure angle from one of the poles, say p_2. We have

- $\alpha_{p_1 \to p_2} = \text{arctan2}(2 - 4.2, -1 + 1.5) \simeq -1.35\,\text{rad}$;
- $\alpha_{p_3 \to p_2} = \text{arctan2}(2 + 2, -1 + 1) = \pi/2\,\text{rad}$;
- $\alpha_{p_4 \to p_2} = \text{arctan2}(2 + 4.2, -1 + 1.5) \simeq 1.49\,\text{rad}$;
- $\alpha_{p_4 \to p_2} = \text{arctan2}(2 - 0, -1 + 0.5) \simeq 1.82\,\text{rad}$.

Thus

$$\alpha_{\text{dep}}(p_2) \simeq \pi + 1.35 - \pi/2 - 1.49 + 1.82 \simeq 3.24\,\text{rad} \simeq 186\,\text{degrees}.$$

Fig. 2.9 illustrates the above calculations.

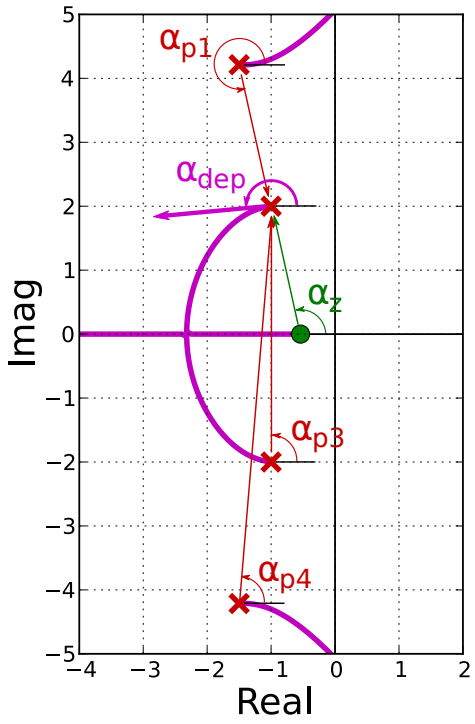

Figure 2.9: Departure angle from a complex pole.

2.2.5 Break-in/break-out points

Break-in/break-out points are points where two branches meet. It is important to find these points to have an accurate drawing of the root locus. Consider a break-in/break-out point s. Since two branches meet at s, s must be a *double* root of the CE, which in turn implies that s cancels the CE *and its derivative*, i.e.

$$P(K,s) = 0 \quad \text{and} \quad P'(K,s) = 0. \tag{2.3}$$

Since $P(K,s) = KN(s) + D(s)$, we have $P'(K,s) = KN'(s) + D'(s)$. From (2.3), we have

$$KN(s) + D(s) \quad \text{and} \quad KN'(s) + D'(s),$$

i.e.

$$\frac{D(s)}{N(s)} = -K = \frac{D'(s)}{N'(s)},$$

which finally yields

$$N'(s)D(s) - D'(s)N(s) = 0.$$

Remark that the above equation is a polynomial equation which does not contain K. It can then be solved to find n roots, $s_1,\ldots,s_n$, which are candidates to be break-in/break-out points. To verify whether any of these roots, say s_i, is indeed a break-in/break-out point, we need to compute the corresponding K by

$$K = -\frac{D(s_i)}{N(s_i)},$$

and verify that this K is real positive. Example 8 illustrates the whole process through a numerical example.

Example 8. Consider again the CE

$$K(s+0.5) + (s^2+2s+5)(s^2+3s+20) = 0.$$

Computing $N'(s)D(s) - D'(s)N(s)$ yields

$$(s^4+5s^3+31s^2+55s+100) - (4s^3+15s^2+62s+55)(s+0.5)$$

$$= -3s^4 - 12s^3 - 38.5s^2 - 31s + 72.5.$$

The above polynomial has 4 roots, which are $s_{1,2} = -1.3 \pm 3.1j$, $s_3 = -2.3$ and $s_4 = 0.9$. Substituting these values of s into

$$K = -\frac{(s^2+2s+5)(s^2+3s+20)}{s+0.5},$$

we find out that $s_{1,2}$ correspond to $K = 3.3 \pm 14.7j$, s_3 to $K = 58.1$ and s_4 to $K = -127.8$. Thus, there is only one break-in/break-out point at $s_3 = -2.3$ and for $K = 58.1$. Fig. 2.6 confirms this result.

2.2.6 Crossing of imaginary axis

A point on the imaginary axis is given by $s = j\omega$. Pluging in

$$KN(j\omega) + D(j\omega) = 0.$$

By separating the real and complex parts, one can find K and ω.

This is important since it indicates when the system becomes unstable: crossing the imaginary axis means that the root locus goes into the RHP, which in turn means that the system becomes unstable.

Example 9. Consider again the CE

$$K(s+0.5) + (s^2+2s+5)(s^2+3s+20) = 0.$$

Letting $s = j\omega$, one obtains

$$K(j\omega+0.5) + [(j\omega)^2+2(j\omega)+5)][(j\omega)^2+3(j\omega)+20] = 0.$$

$$j[-5\omega^3 + (55+K)\omega] + [\omega^4 - 31\omega^2 + 100 + 0.5K] = 0.$$

One thus have

$$\begin{cases} -5\omega^3 + (55+K)\omega &= 0 \\ \omega^4 - 31\omega^2 + 100 + 0.5K &= 0 \end{cases}$$

The first equation yields

$$K = 5\omega^2 - 55. \tag{2.4}$$

Substituting this expression of K into the second equation yields

$$\omega^4 - 28.5\omega^2 + 72.5 = 0,$$

which has four solutions $\omega = \pm 1.68$ or $\omega = \pm 5.07$.

From (2.4), we find that the solutions $\omega = \pm 1.68$ correspond to $K = -40.9$ and the solutions $\omega = \pm 5.07$ correspond to $K = 73.4$. We can thus conclude that the root locus cross the imaginary axis for $\omega = \pm 5.07$ and $K = 73.4$.

The gain K where the system crosses the imaginary axis can also be recovered by the Routh-Hurwitz criterion.

Example 10. Consider the same CE as in the previous example

$$K(s+0.5) + (s^2+2s+5)(s^2+3s+20) = 0.$$

Expanding this CE yields

$$s^4 + 5s^3 + 31s^2 + (55+K)s + (100+0.5K) = 0.$$

Construct the Routh array

s^4	1	31	$100+0.5K$
s^3	5	$55+K$	
s^2	$\frac{100-K}{5}$	$100+0.5K$	
s	$\frac{-K^2+32.5K+3000}{100-K}$	0	
1	$100+0.5K$		

The first column of the Routh array gives the following necessary and sufficient condition for stability: $K < 100$ and $K^2 - 32.5K - 3000 < 0$. The latter inequality yields $-40.9 < K < 73.4$. Therefore, the necessary and sufficient condition for stability is that $K < 73.4$. We have thus recovered the result of Example 9.

2.2.7 Summary

Summary 3. To sketch the root locus of a CE given in the form $KN(s) + D(s) = 0$, take the following steps

1. Compute the poles (roots of D) and the zeros (roots of N);
2. Determine the number of infinite branches ($=n_{\text{poles}} - n_{\text{zeros}}$), which gives the number and configuration of the asymptotes. Compute the intersection point σ_a of the asymptotes by
$$\sigma_a = \frac{\sum \text{poles} - \sum \text{zeros}}{n_{\text{poles}} - n_{\text{zeros}}};$$
3. Determine the locus on the real axis by considering the real poles and zeros;
4. For each complex pole (resp. zero), compute the departure (resp. arrival) angle by
$$\alpha_{\text{dep}}(p) = \pi - \sum_{\text{poles } p_i} \alpha_{p_i \to p} + \sum_{\text{zeros } z_i} \alpha_{z_i \to p}.$$
$$\alpha_{\text{arr}}(z) = \pi + \sum_{\text{poles } p_i} \alpha_{p_i \to z} - \sum_{\text{zeros } z_i} \alpha_{z_i \to z}.$$
5. Determine the break-in/break-out points by solving
$$N'(s)D(s) - D'(s)N(s) = 0;$$
6. Determine the crossing of the imaginary axis by solving
$$KN(j\omega) + D(j\omega) = 0;$$
7. Based on all the information obtained so far, sketch the root locus.

2.3 Transient response design by gain adjustment

We have seen that the transient behavior depends on the locations of the dominant (rightmost) poles : given performance specifications (in terms of maximum overshoot, settling time, etc.), we can calculate the desired damping coefficient ζ and undamped natural frequency ω_n, which in turn yield the desired locations for the dominant pole(s) s_{desired}.

If s_{desired} is on the root locus, then it means that gain adjustment (i.e. varying K) alone is sufficient to set s_{desired} as system pole. To verify whether s_{desired} is on the root locus, we can either see graphically, or use the angle

criterion as follows.

Assume that s_{desired} is on the root locus. Then, there exists a K such that $KN(s_{\text{desired}}) + D(s_{\text{desired}}) = 0$, i.e.

$$\frac{D(s_{\text{desired}})}{N(s_{\text{desired}})} = -K,$$

which implies

$$\angle \frac{D(s_{\text{desired}})}{N(s_{\text{desired}})} = \angle(-K) = \pi.$$

Thus, if

$$\angle D(s_{\text{desired}}) - \angle N(s_{\text{desired}}) = \pi \mod 2\pi^{1}, \tag{2.5}$$

then the root locus goes through s_{desired}.

Next, *if* the root locus indeed goes through s_{desired}, then one can determine the corresponding gain K by

$$K = \frac{\|D(s_{\text{desired}})\|}{\|N(s_{\text{desired}})\|}.$$

Example 11. Consider the CE of the helicopter system with PD control [cf. Equation 2.1 in Section 2.1], which can be rewritten as (for $m = 2$, $k = 0.5$)

$$K[0.5(s+1)] + 2s^2 = 0.$$

Let us examine whether the root locus goes through $s_0 = -2 + j$ and $s_1 = -1 + j$, and if it does, determine the corresponding gain K.

Applying the angle criterion for s_0

$$\begin{aligned}
\angle D(s_0) - \angle N(s_0) &= \angle[2(-2+j)^2] - \angle[0.5(-2+j+1)] \\
&= \angle[(-2+j)^2] - \angle[(-2+j+1)] \\
&= 2\angle(-2+j) - \angle(-1+j) \\
&= 2[\pi - \arctan(0.5)] - \frac{3\pi}{4} \\
&\sim 3.0 \neq \pi \mod 2\pi.
\end{aligned}$$

Thus, s_0 is *not* on the root locus.

Applying the angle criterion for s_1

$$\begin{aligned}
\angle D(s_1) - \angle N(s_1) &= \angle[(-1+j)^2] - \angle(-1+j+1) \\
&= 2\angle(-1+j) - \angle j = \frac{3\pi}{2} - \frac{\pi}{2} = \pi.
\end{aligned}$$

Thus, s_1 is on the root locus.

[1] "$\alpha = \beta \mod 2\pi$" means : there exists an integer k, such that $\alpha = \beta + 2k\pi$. For example, $\frac{pi}{4} = \frac{5\pi}{4} \mod 2\pi = \frac{5\pi}{4} \mod 2\pi$, etc.

Next, we can compute the gain K that corresponds to s_1 by

$$K = \frac{\|2(-1+j)^2\|}{\|0.5(-1+j+1)\|} = \frac{4}{0.5} = 8.$$

One can verify these results graphically in Fig. 2.2.

Finally, in case the system has zeros and/or is of order > 2, we have to make sure the second-order approximation is valid for the value of K just found. For this, we plug the value of K into the CE, evaluate the remaining poles, and verify that (see part I of the course for more details)

- non-dominant poles are far to the left;
- zeros are far to the left;
- zeros that are not far to the left are cancelled by poles (pole/zero cancellation).

If necessary, we may simulate the response using Matlab/Python and verify that the specifications are met.

2.4 Improving transient behavior by lead compensation

Section 2.3 addressed the case when the desired pole location s_{desired} is on the root locus. If this is not the case, then one needs to *reshape* the root locus and force it to go through s_{desired}. There are two main ways to do so, either with a *PD controller* or with a *lead compensator* (in fact, PD controllers can be seen as idealized versions of lead compensators).

2.4.1 PD controller

We have seen (e.g. in Fig. 1.1.3) that a PD controller can be represented as a block $(K_D s + K_P)$ inserted before the system to be controlled. This can be rewritten

$$K_D s + K_P = K_D \left(s + \frac{K_P}{K_D} \right) = K(s + z_c),$$

where $K = K_D$ and $z_c = \frac{K_P}{K_D}$. Consider now a system with and without PD control.

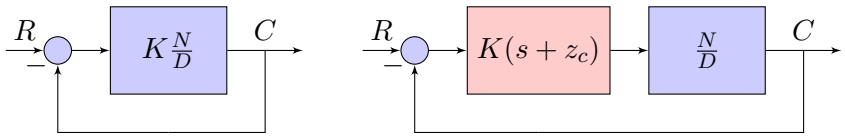

Figure 2.10: Left: system without PD control. Right: system with PD control.

The CE for the system *without PD* control is

$$KN(s) + D(s) = 0.$$

The fact that the root locus of this system does *not* go through s_{desired} means that the angle criterion (2.5) is not satisfied, i.e.

$$\angle D(s_{\text{desired}}) - \angle N(s_{\text{desired}}) \neq \pi \mod 2\pi.$$

The CE of the system *with PD* control is

$$K(s + z_c)N(s) + D(s) = 0.$$

Since we want the root locus of the new system to go through s_{desired}, we substitute s_{desired} into the CE

$$K(s_{\text{desired}} + z_c)N(s_{\text{desired}}) + D(s_{\text{desired}}) = 0.$$

As the value of s_{desired} is given, the above equation has only two unknowns, K and z_c. Examining the real and imaginary parts of the equation yields two independent equations, which allows solving for K and z_c. Finally, the proportional and derivative gains are finally given by

$$K_D = K, \quad K_P = z_c K.$$

Example 12 shows the method in action.

Example 12. Consider the system below. We would like to design a PD controller so that $s_{\text{desired}} = -2 \pm 1.9j$ are root of the system.

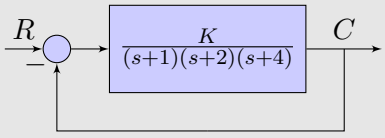

The root locus of this system is given Fig. 2.11.

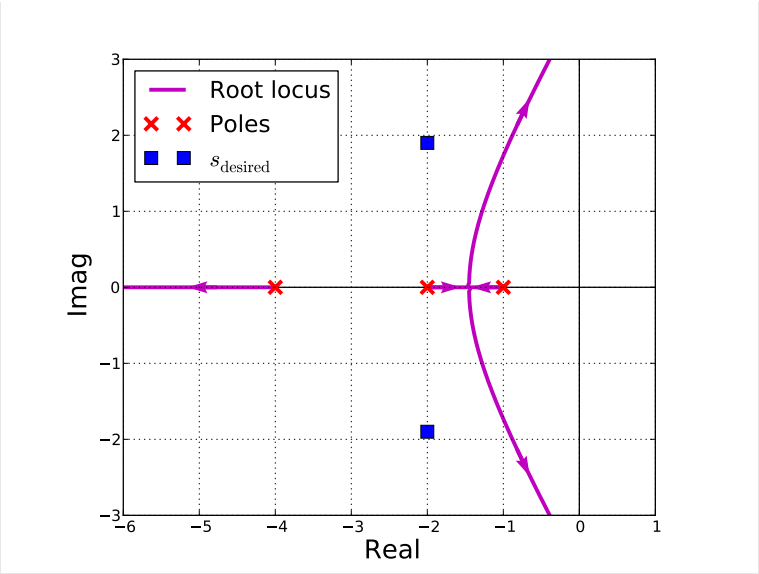

Figure 2.11: Root locus of the uncompensated system.

Clearly, the root locus does not go through $s_{\text{desired}} = -2 \pm 1.9j$. To verify this, we apply the angle criterion

$$\angle D(s_{\text{desired}}) - \angle N(s_{\text{desired}}) = \angle[(-2+1.9j+1)(-2+1.9j+2)(-2+1.9j+4)]$$

$$= \angle(-3.61 - 10.66j) \simeq 4.38\,\text{rad} \neq \pi.$$

We want now to find K and z_c such that

$$K(s_{\text{desired}} + z_c)N(s_{\text{desired}}) + D(s_{\text{desired}}) = 0.$$

Substituting $s_{\text{desired}} = -2 + 1.9j$ yields

$$K(-2+1.9j+z_c)+(-2+1.9j+1)(-2+1.9j+2)(-2+1.9j+4) = 0, \quad \text{i.e.}$$

$$[-3.61 - (2 - z_c)K] - [10.66 - 1.9K]j = 0. \tag{2.6}$$

The imaginary part of (2.6) yields

$$K = \frac{10.66}{1.9} = 5.61.$$

Substituting $K = 5.61$ in the real part of (2.6) yields

$$2 - zc = \frac{-3.61}{5.61} = -0.64, \quad \text{i.e.} \quad z_c = 2 + 0.64 = 2.64.$$

Finally,

$$K_D = K = 5.61, \quad K_P = z_c K = 14.83.$$

The compensated system is thus given by

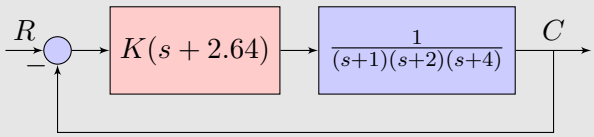

The root locus of the compensated system is given in Fig. 2.12. We can see that the root locus indeed goes through $s_{\text{desired}} = -2 \pm 1.9j$ for $K = 5.61$.

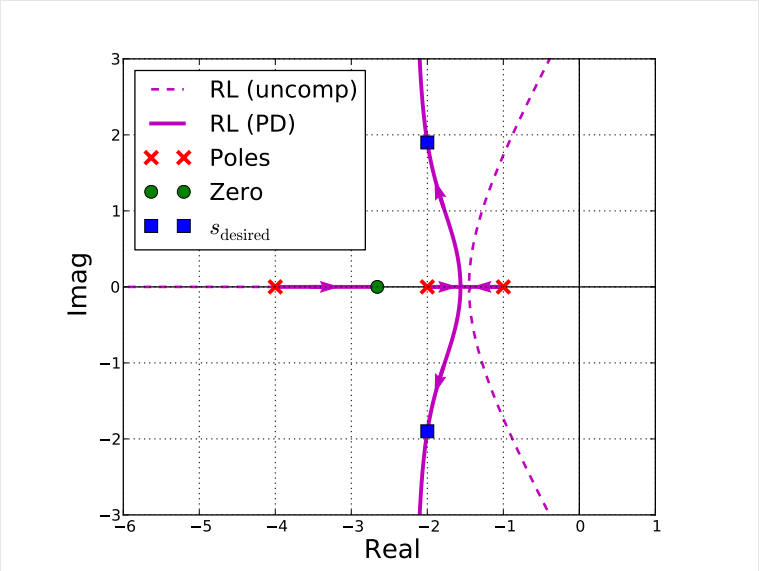

Figure 2.12: System compensated with PD controller.

2.4.2 Lead compensator

We have seen that PD controllers were able to force the root locus to go through almost arbitrary desired root locations. However, there are two main drawbacks with PD controllers

- PD controllers cannot be realized via *passive* circuits (mass-spring-dampers for mechanical systems, resistor-inductor-capacitor for electronic circuits): additional power must be provided by *active* components, such as operational amplifiers;
- PD controllers are sensitive to noise (see below).

One way to address these drawbacks consists in using *lead compensators*. A lead compensator is a block with transfer function $K\frac{s+z_c}{s+p_c}$ that is inserted before the system to be controlled. We can see that a lead compensator is similar to a PD controller, except for the term $1/(s+p_c)$.

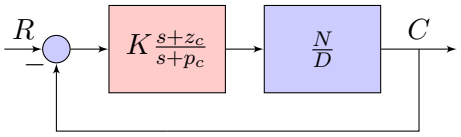

Figure 2.13: System with lead compensator.

The CE of the system with lead compensator becomes

$$K(s+z_c)N(s)+(s+p_c)D(s)=0.$$

Since we want the root locus of the new system to go through s_{desired}, we substitute s_{desired} into the CE

$$K(s_{\text{desired}}+z_c)N(s_{\text{desired}})+(s_{\text{desired}}+p_c)D(s_{\text{desired}})=0. \tag{2.7}$$

As the value of s_{desired} is given, the above equation has three unknowns, K, z_c and p_c. Examining the real and imaginary parts of the equation yields two independent equations. Two equations and three unknowns means that, contrary to the PD controller case, there are *multiple* values of K, z_c and p_c that can satisfy (2.7). However, if we fix a particular value for z_c, then K and p_c will be uniquely determined. In practice, we shall choose a sensible value for z_c, and then determine the corresponding values for K and p_c, as shown in Example 13.

Example 13. Consider the same system as in Example 12. We shall design a lead compensator so that $s_{\text{desired}}=2\pm 1.9j$ are roots of the system.

First of all, we compute the z_c^* that corresponds to the PD controller. We saw in Example 12 that the this value is $z_c^*=2.64$. The possible (and desirable) values for z_c will be smaller than that critical value, yielding less derivation.

As stated in the main text, there are multiple possible values for z_c: in fact, any z_c verifying $0<z_c<z_c^*$ is possible. Let fix $z_c=1.5$ and study how we can compute the corresponding p_c.

Substituting $s_{\text{desired}}=-2+1.9j$ and $z_c=1.5$ in (2.7) yields

$$K(-2+1.9j+1.5)+$$

$$(-2+1.9j+p_c)(-2+1.9j+1)(-2+1.9j+2)(-2+1.9j+4)=0, \quad \text{i.e.}$$

$$[27.47-3.61p_c-0.5K]-[14.46-10.66p_c+1.9K]j=0. \tag{2.8}$$

We thus have the following 2×2 linear system

$$\begin{cases} -3.61p_c - 0.5K &= -27.47 \\ -10.66p_c + 1.9K &= -14.46 \end{cases},$$

which yields the solution $p_c = 4.88$, $K = 19.74$.

As stated in the main text, different values of z_c will yield different values of p_c and K. For example,

- If $z_c = 1$, we shall find $p_c = 3.80$ and $K = 13.74$;
- If $z_c = 0.5$, we shall find $p_c = 3.23$ and $K = 10.53$.

The following figures plot the root locus for the three cases.

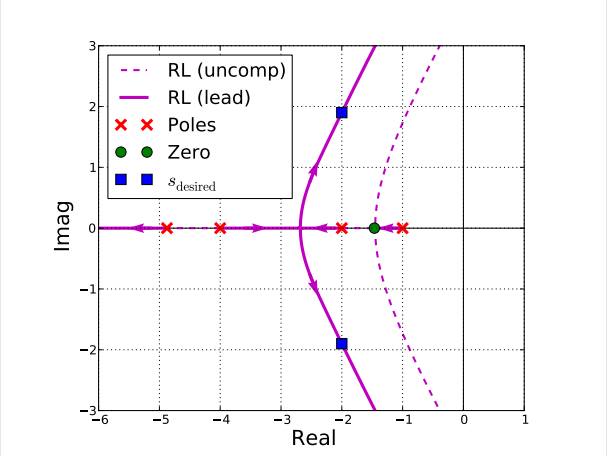

Figure 2.14: System with lead compensation $\frac{s+1.5}{s+4.88}$.

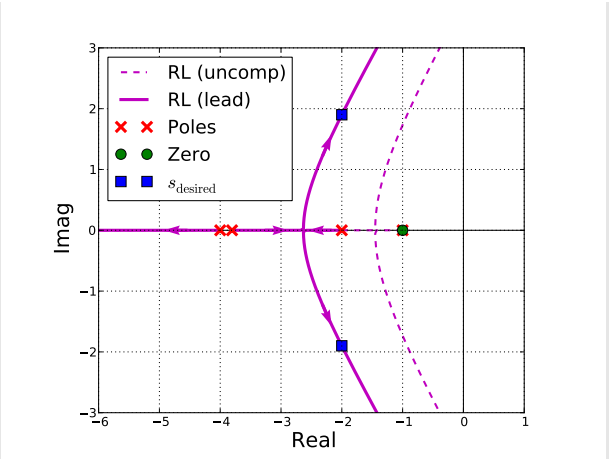

Figure 2.15: System with lead compensation $\frac{s+1}{s+3.80}$.

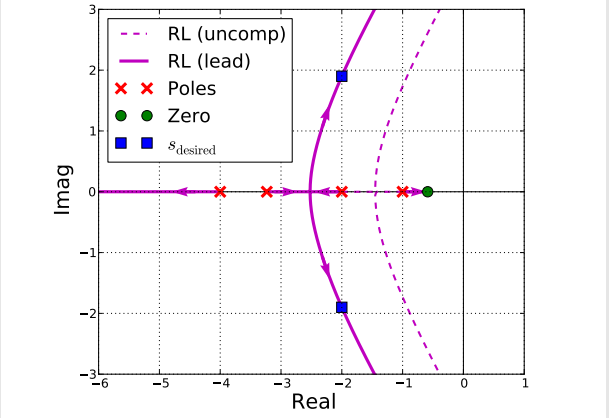

Figure 2.16: System with lead compensation $\frac{s+0.5}{s+3.23}$.

Let us now compare the steady-state errors to unit step input of the different compensated sytems (which are all of type 0).

Recall first that the position constant [a] is given by

$$K_p = \lim_{s\to 0} K(s+z_c)\frac{N(s)}{D(s)} = \frac{Kz_c}{8}$$

and

$$K_p = \lim_{s\to 0} K\frac{s+z_c}{s+p_c}\frac{N(s)}{D(s)} = \frac{Kz_c}{8p_c}$$

for the PD controller and the lead compensators respectively. The

steady-state error for unit step input is then given by

$$e_{\text{ss}} = \frac{1}{1 + K_p}.$$

	PD control	Lead comp 1	Lead comp 2	Lead comp 3
z_c	2.64	1.5	1	0.5
p_c	NA	4.88	3.80	3.23
K	5.61	19.74	13.74	10.53
K_p	1.85	0.76	0.45	0.20
e_{ss}	0.35	0.57	0.69	0.83

We can observe that the PD controller yields the best steady-state behavior, and that steady-state performance of the lead compensators decreases as z_c becomes smaller, i.e. as they grow further away from the PD controller, their ideal representative.

The choice of the appropriate lead compensator in a particular application will ultimately depend on a trade-off among many factors, including

- goodness of second-order approximation;
- desired steady-state error;
- sensitivity to noise;
- ease of implementation with physical components,...

[a] Note that the position constant K_p and the proportional gain K_P are two different objects.

Let us now explain why lead compensators are less sensitive to noise than PD controllers. Basically, noise is a signal with very high frequency. We shall see in Chapter 3 that the amplitude of the response of a system with transfer function G to a signal of frequency ω is given by $\|G(j\omega)\|$. Thus, the amplitude of the response of a PD controller is $\|K(j\omega + z_c)\|$, which converges to ∞ ans $\omega \to \infty$. On the other hand, the amplitude of the response of a lag compensator is

$$\frac{K\|j\omega + z_c\|}{\|j\omega + p_c\|},$$

which converges to K as $\omega \to \infty$.

2.5 Reducing steady-state error by lag compensation

Suppose that the original system has a good transient behavior, but its steady-state error does not meet the specifications. The idea here thus consists in improving the steady-state error *without* changing noticeably the root locus, thereby preserving the transient behavior. There are two main ways to do so, either with a *PI controller* or with a *lag compensator* (in fact, PI controllers can be seen as idealized versions of lag compensators).

2.5.1 PI controller

A PI controller can be represented as a block $(K_P + \frac{K_I}{s})$ inserted before the system to be controlled. This can be rewritten as

$$K_P + \frac{K_I}{s} = \frac{K_P s + K_I}{s} = \frac{K_P \left(s + \frac{K_I}{K_P}\right)}{s} = \frac{K(s + z_c)}{s}$$

where $K = K_P$ and $z_c = \frac{K_I}{K_P}$. Consider now a type-1 system with and without PI control.

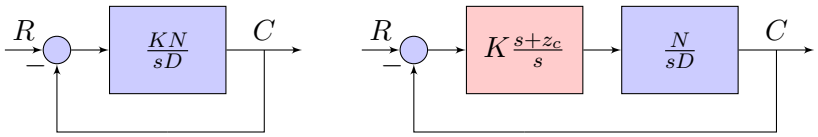

Figure 2.17: Left: type-1 system without PI control (note that N and D must contain no "s" term for the system to be of type 1). Right: the same system with PI control.

Since the original system is of type 1, it has 0 steady-state error to step input. For ramp input, let us compute the *velocity constant*

$$K_v = \lim_{s\to 0} sK\frac{N(s)}{sD(s)} = \frac{KN(0)}{D(0)}.$$

Note that $N(0) \neq 0$ and $D(0) \neq 0$ since N and D do not contain any "s" term.

Next, the steady-state error to ramp input is given by

$$e_{\text{ss}} = \frac{1}{K_v} = \frac{D(0)}{KN(0)} \neq 0. \tag{2.9}$$

For the system with PI control, we have

$$K_v = \lim_{s\to 0} sK\frac{s + z_c}{s}\frac{N(s)}{sD(s)} = \lim_{s\to 0}\frac{KN(0)}{sD(0)} = \infty.$$

Thus, the steady-state error to ramp input of the system with PI control is given by

$$e_{\text{ss}} = \frac{1}{K_v} = 0.$$

Thus, PI control enables cancelling the steady state error to ramp inputs for type-1 systems. A similar reasoning applies to step inputs and type-0 systems, parabolic inputs and type-2 systems, etc.

In fact, as can be seen directly from the block diagram, the PI controller increases the type of a given system by 1 (type-0 systems become type-1, type-1 systems become type-2, etc.)

Let us now examine how the PI controller affects the transient behavior. Adding the PI controller amounts to adding a new pole at $s = 0$ and a new zero at $s = -z_c$. Thus, if z_c is very small, then the new pole and new zero will *cancel* each other, leaving the root locus, hence the transient behavior, almost unchanged.

Example 14. Consider the system below. We would like to design a PI controller that eliminates steady-state error to ramp inputs without changing the transient behavior.

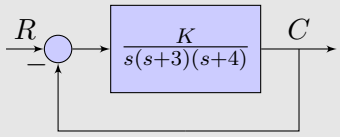

First, we sketch the root locus of this system in Fig. 2.18.

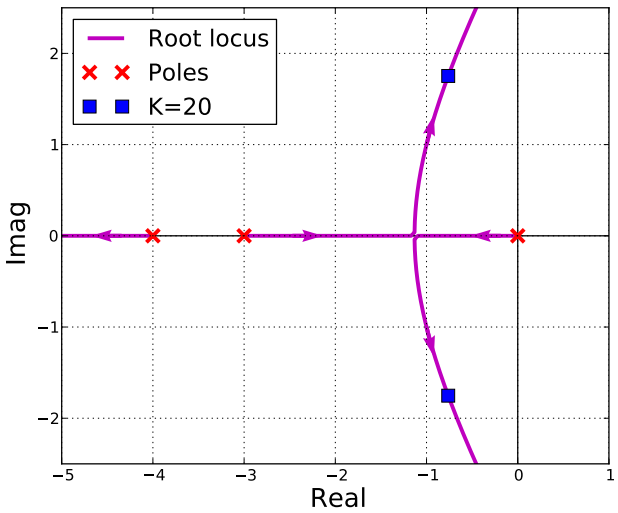

Figure 2.18: Root locus of the uncompensated system.

Assume that the desired transient behavior of this system corresponds the roots $s_{\text{desired}} = -0.76 \pm 1.75j$ and achieved for $K = 20$.

Next, the velocity constant and the steady-state error to unit ramp intput are given by

$$K_v = \lim_{s\to 0} sK \frac{1}{s(s+3)(s+4)} = \frac{20}{12} = \frac{5}{3},$$

$$e_{\text{ss}} = \frac{1}{K_v} = \frac{3}{5} = 0.6.$$

Consider now two PI controllers with $z_c = 0.2$ and $z_c = 0.1$. The root loci of the two compensated systems are given in Fig. 2.19 and Fig. 2.20.

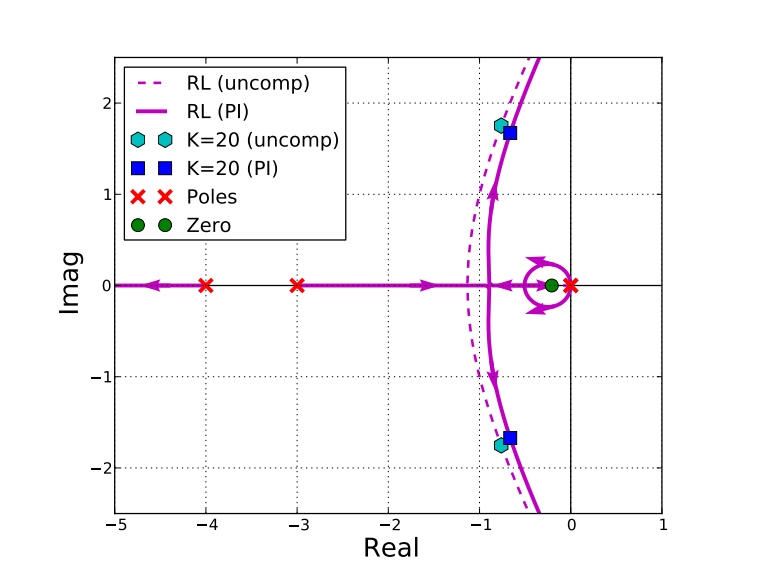

Figure 2.19: System compensated with PI controller ($z_c = 0.2$).

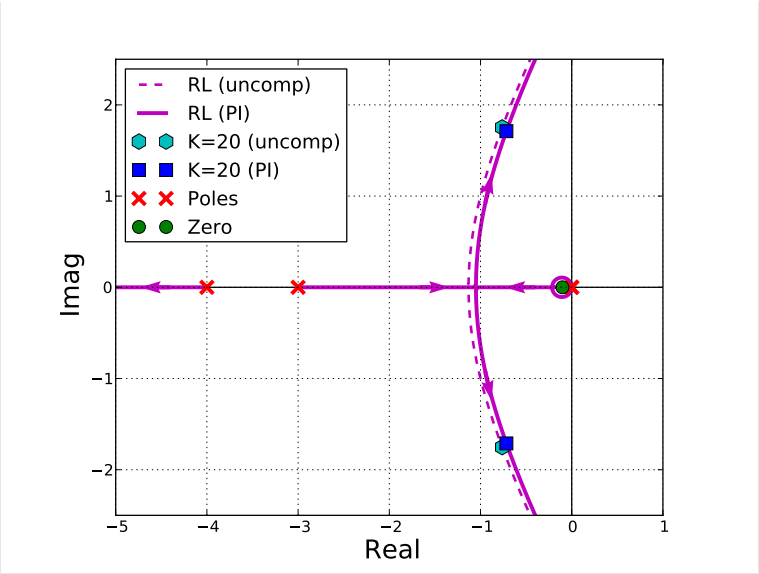

Figure 2.20: System compensated with PI controller ($z_c = 0.1$).

From the theoretical analysis in the main text, the steady-state error to ramp inputs becomes 0. At the same time, we can observe that the root locus changes a bit for $z_c = 0.2$ and very little for $z_c = 0.1$. In fact, for $z_c \to 0$, the root locus will become identical to that of the original system.

In particular, the poles of the PI-controlled system for $K = 20$ are given by

- $\{-5.45, -0.66 \pm 1.67j, -0.23\}$ for $z_c = 0.2$;
- $\{-5.46, -0.72 \pm 1.71j, -0.11\}$ for $z_c = 0.1$.

Thus, as z_c becomes smaller, the dominant pole will get closer to z_c, yielding a better pole/zero compensation, while the two complex poles with get closer to $s_{\text{desired}} = -0.76 \pm 1.75j$.

To illustrate the above development, we plot the response of the original system and the compensated systems to unit step and ramp inputs in Fig. 2.21. We can see that the step response of the compensated systems are similar to the original system while the ramp error is reduced from 0.6 in the original system to 0 in the compensated systems.

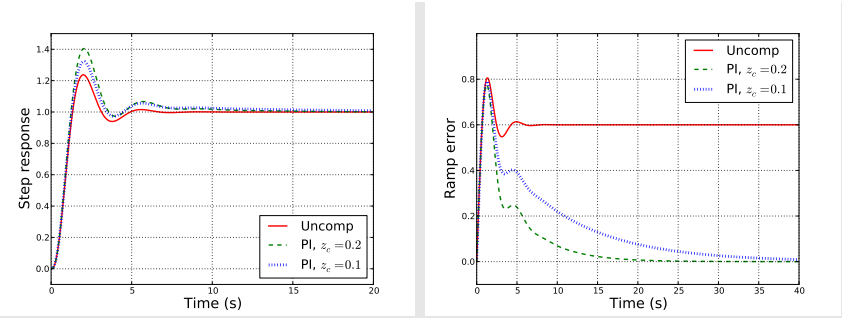

Figure 2.21: Left: response to unit step. Right: error to unit ramp.

2.5.2 Lag compensator

PI controllers, as PD controllers, cannot be realized by passive components. Thus, similarly to lead compensators, which approximate PD controllers, we introduce here lag compensators, which approximate PI controllers, but which can be realized by passive components.

Recall that PI controllers are basically a block with transfer function $K\frac{s+z_c}{s}$ where z_c is very small. Lag compensators are given by the transfer function $K\frac{s+z_c}{s+p_c}$ where z_c and p_c are very small, and p_c is very small compared to z_c. Consider the same type-1 system as previously, now with a lag compensator.

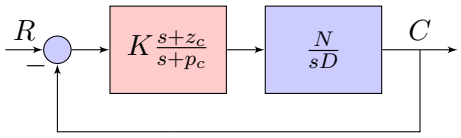

Figure 2.22: Type-1 system with lag compensation.

Compute again the velocity constant and the steady-state error to unit ramp input for the compensated system

$$K_v = \lim_{s\to 0} sK\frac{s+z_c}{s+p_c}\frac{N(s)}{sD(s)} = \lim_{s\to 0}\frac{KN(0)}{D(0)}\frac{z_c}{p_c},$$

$$e_{\text{ss}} = \frac{1}{K_v} = \frac{D(0)}{KN(0)}\frac{p_c}{z_c}.$$

Thus, the steady-state error has been reduced by a factor $\frac{p_c}{z_c}$ as compared to the uncompensated system (2.9). Thus, if $p_c \ll z_c$, then the steady-state error can become very small.

Regarding the transient behavior, if both p_c and z_c are very close to zero, then we shall have pole/zero cancellation. Thus, the root locus of the system will be changed very little.

Example 15. Consider the same system as in Example 12. We would like to design a lag compensator to reduce the steady-state error by a factor 4 without changing noticeably the transient behavior.

We choose $p_c = 0.05$ and $z_c = 0.2$ so that $\frac{p_c}{z_c} = \frac{1}{4}$ and p_c and z_c are small enough. The root locus is given in Fig. 2.23 and Fig. 2.24. We can observe that the root locus has been changed a little.

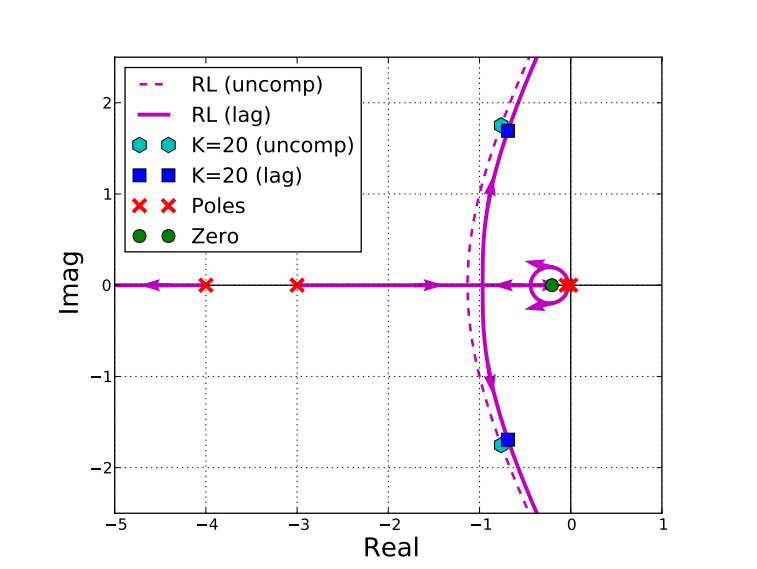

Figure 2.23: Root locus of the system with lag compensation.

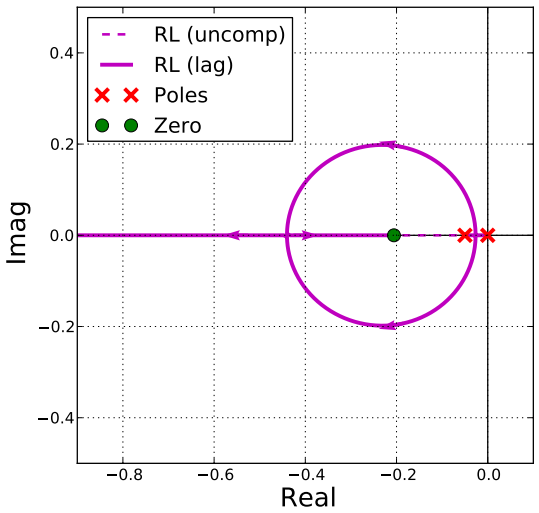

Figure 2.24: Zoomed in near 0.

Note that we could also choose $p_c = 0.005$ and $z_c = 0.02$, which would give us the same reduction in terms of steady-state error but which would yield a root locus even closer to the original one. In fact, there are infinitely many ways to choose these values. Ultimately, the choice of the appropriate lag compensator in a particular application will ultimately depend on a trade-off among many factors, including

- stability of the compensated system;
- desired steady-state error;
- closeness to original root locus;
- ease of implementation with physical components,...

2.6 Improving transient behavior *and* reducing steady-state error

To improve both transient behavior *and* reducing steady-state error, we can combine PD and PI controllers into a PID controller (ideal case) or we can combine lead and lag compensators into a lead-lag compensator (realizable with passive components).

2.6.1 PID controller

Consider a system with feedforward transfer function $G(s)$. We first design a PD controller $K_1(s + z_{c1})$ to meet the transients specifications. Then, we design a PI controller $K_2\frac{s+z_{c2}}{s}$ for the system with feedforward TF $K_1(s + z_{c1})G(s)$ to meet the steady-state specifications without noticeably changing the transient behavior achieved previously. The resulting system will have a feedforward TF given by

$$K_2\frac{s + z_{c2}}{s}K_1(s + z_{c1})G(s).$$

The TF of the PID controller can also be rewritten as

$$K_1K_2\left(s + (z_{c1} + z_{c2}) + \frac{z_{c1}z_{c2}}{s}\right) = K_Ds + K_P + \frac{K_I}{s},$$

where $K_D = K_1K_2$, $K_P = K_1K_2(z_{c1} + z_{c2})$, and $K_I = K_1K_2z_{c1}z_{c2}$.

2.6.2 Lead-lag compensator

Here, we first design a lead compensator $K_1\frac{s+z_{c1}}{s+p_{c1}}$, with $p_{c1} > z_{c_1}$, to meet the transients specifications. Then, we design a lag compensator $K_2\frac{s+z_{c2}}{s+p_{c2}}$, with $p_{c1} < z_{c_1} \ll 1$, for the lead-compensated system to meet the steady-state specifications without noticeably changing the transient behavior achieved previously. The resulting system will have a feedforward TF given by

$$K_2\frac{s + z_{c2}}{s + p_{c2}}K_1\frac{s + z_{c1}}{s + p_{c1}}G(s) = K_1K_2\frac{(s + z_{c1})(s + z_{c2})}{(s + p_{c1})(s + p_{c2})}G(s).$$

Furthermore, if $\frac{z_{c1}}{p_{c1}} = \frac{p_{c2}}{z_{c2}}$, the TF of the lead-lag compensator can be rewritten as

$$K\frac{(s + \frac{1}{T_1})(s + \frac{1}{T_2})}{(s + \frac{1}{\alpha T_1})(s + \frac{\alpha}{T_2})},$$

where $K = K_1K_2$, $T_1 = \frac{1}{z_{c1}}$, $T_2 = \frac{1}{z_{c2}}$, $\alpha = \frac{z_{c1}}{p_{c1}} = \frac{p_{c2}}{z_{c2}} > 1$.

2.7 Physical implementation of compensators

2.7.1 Lead compensators

Consider the electrical circuit in Fig. 2.25. Its transfer function is given by

$$\frac{V_o}{V_i} = \frac{s + \frac{1}{R_1C}}{s + \frac{1}{R_1C} + \frac{1}{R_2C}}.$$

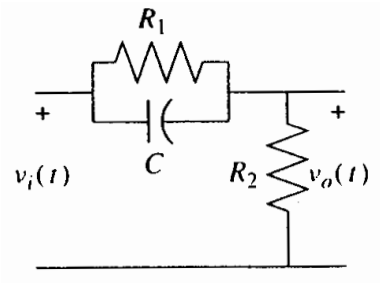

Figure 2.25: Electrical implementation of a lead compensator.

Thus, given desired z_c and p_c, we can choose R_1, R_2 and C such that

$$R_1 C = \frac{1}{z_c}, \quad R_2 C = \frac{1}{p_c - z_c}.$$

Note that the amplification gain K still needs to be realized by an active element.

2.7.2 Lag compensators

Consider the electrical circuit in Fig. 2.26. Its transfer function is given by

$$\frac{V_o}{V_i} = \frac{R_2}{R_1 + R_2} \frac{s + \frac{1}{R_2 C}}{s + \frac{1}{(R_1 + R_2)C}}.$$

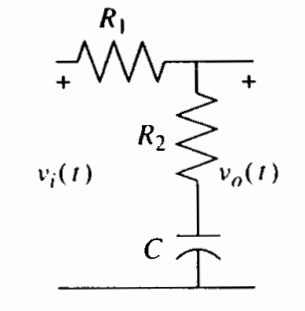

Figure 2.26: Electrical implementation of a lag compensator.

Thus, given desired z_c and p_c, we can choose R_1, R_2 and C such that

$$R_1 C = \frac{1}{z_c}, \quad R_2 C = \frac{1}{p_c} - \frac{1}{z_c}.$$

Note that the amplification gain K still needs to be realized by an active element.

2.8 Parallel compensation

Up to now, we have considered *series* controllers/compensators, which are inserted in series before the system. It is also possible to perform *parallel* compensation by placing a new element in a *minor feedback loop* in parallel with the system.

Consider the same generic unit feedback system as in Fig. 2.5.2 but now with parallel compensation.

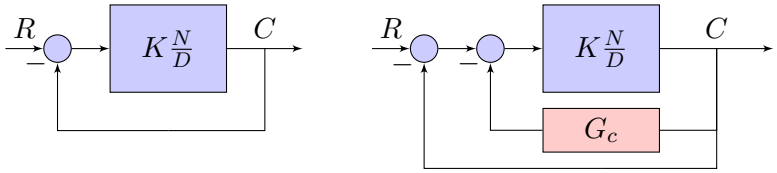

Figure 2.27: Left: original system. Right: system with parallel compensation.

The transfer function of the internal loop is given by

$$\frac{K\frac{N}{D}}{1+G_c\frac{N}{D}} = \frac{KN}{D+KG_cN}.$$

Thus, the transfer function of the full compensated system is given by

$$\frac{C}{R} = \frac{\frac{KN}{D+KG_cN}}{1+\frac{KN}{D+KG_cN}} = \frac{KN}{KN+D+KG_cN}.$$

The CE of the system is then

$$KN(1+G_c)+D=0.$$

Assume now that G_c has the form $G_c = K_c s$, then the CE becomes

$$KN(1+K_cs)+D=0, \quad \text{i.e.}$$

$$\tilde{K}N(s+z_c)+D=0, \tag{2.10}$$

where $\tilde{K} = KK_c$ and $z_c = 1/K_c$.

We can remark now that equation 2.10 is the same as the CE of a system with PD control. Thus, using the same technique as in Section 2.4.1 will enable us to achieve desired transient behaviors.

Example 16. Consider the system in Example 12. We would like to design a velocity feedback (or tachometer feedback) controller so that $s_{\text{desired}} = -2 \pm 1.9j$ are root of the system.

The system with velocity feedback is given by

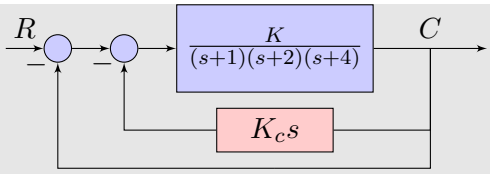

Following the development in the main text, s_{desired} is root of the system if

$$\tilde{K}N(s_{\text{desired}})(s_{\text{desired}} + z_c) + D(s_{\text{desired}}) = 0.$$

We had the same equation in Example 12, which yielded $z_c = 2.64$ and $\tilde{K} = 5.61$. Thus, the velocity feedback gain and the feedforward gain of the system at hand are given by

$$K_c = 1/z_c = 0.38, \quad K = \tilde{K}/K_c = 14.8.$$

2.9 Summary

Summary 4. The main functions of different controllers/compensators are summarized below.

- To improve transient behavior, we can use either PD controllers or lead compensators.
  - PD controllers require active components to implement and are sensitive to noise;
  - lead compensators can be implemented by passive components only and are less sensitive to noise.
- To reduce steady-state error, we can use either PI controllers or lag compensators.
  - PI controllers require active components to implement;
  - lag compensators can be implemented by passive components only.
- To improve transient behavior *and* reduce steady-state error, we can use PID controllers or lead-lag compensators.
- Parallel controllers/compensators can be designed by computing the CE and refer to the series controllers/compensators that have the same form of CE.

Chapter 3

Controller design by the frequency response method

3.1 Introduction to frequency response

Up to now we have studied the response of linear systems to step, ramp, parabolic,... inputs. We were interested in the transient behavior as well as the steady-state tracking errors of these systems. In this chapter, we shall take another viewpoint on these systems by studying their responses to *sinusoidal* inputs with various frequencies. This study is important for several reasons, including

- many input signals in real life are periodic (think of pump vibration, alternating current, guitar strings, human walking, etc.) Any periodic signals can be decomposed as a sum of sinusoids. By the superposition principle, the response of the system to a periodic signal can then be found as a sum of the responses to each sinusoids;
- in many engineering problems, the transfer function is unknown. We can nevertheless gain insight into the system experimentally by subjecting the system to sinusoidal inputs of various frequencies and by measuring its responses.

Consider a linear system with transfer function

$$\frac{C}{R} = G(s) = \frac{N(s)}{(s+p_1)\dots(s+p_n)}.$$

Assume that the p_i are distinct (the case with non distinct poles does not present particular difficulties) and that the system is stable, i.e., $\text{Real}(p_i) > 0$ for all i.

Assume that the system is subjected to a sinusoid input of the form

$$r(t) = \sin(\omega t).$$

The Laplace transform of the input is given by

$$R(s) = \frac{\omega}{s^2 + \omega^2}.$$

Thus, the response of the system is given by

$$C(s) = G(s)R(s)$$

$$= \frac{N(s)}{(s+p_1)\dots(s+p_n)} \frac{\omega}{(s^2+\omega^2)} = \frac{\omega N(s)}{(s+j\omega)(s-j\omega)(s+p_1)\dots(s+p_n)}.$$

The partial fraction expansion yields

$$C(s) = \frac{a}{s+j\omega} + \frac{\bar{a}}{s-j\omega} + \frac{b_1}{s+p_1} + \dots + \frac{b_n}{s+p_n}, \tag{3.1}$$

where

$$a = \left.\frac{G(s)\omega(s+j\omega)}{s^2+\omega^2}\right|_{s=-j\omega} = \left.\frac{G(s)\omega}{s-j\omega}\right|_{s=-j\omega} = -\frac{G(-j\omega)}{2j},$$

and $\bar{a}$ is the complex conjugate of a.

Next, the time-domaine response is given by the Laplace inverse transform of (3.1)

$$c(t) = ae^{-j\omega t} + \bar{a}e^{j\omega t} + b_1 e^{-p_1 t} + \dots + b_n e^{-p_n t}.$$

When $t \to \infty$, the terms $b_i e^{-p_i t}$ will vanish (since $\text{Real}(p_i) > 0$), thus the steady-state response is given by

$$c_{\text{ss}}(t) = ae^{-j\omega t} + \bar{a}e^{j\omega t}.$$

Let us next rewrite $G(j\omega)$ in the polar form as $G(j\omega) = \rho e^{i\phi}$, where $\rho = \|G(j\omega)\|$ and $\phi = \angle G(j\omega)$. Thus a and $\bar{a}$ can be rewritten as

$$a = -\frac{\rho e^{-j\phi}}{2j}, \quad \bar{a} = \frac{\rho e^{j\phi}}{2j},$$

which yields

$$c_{\text{ss}}(t) = \rho \frac{e^{j(\omega t+\phi)} - e^{-j(\omega t+\phi)}}{2j} = \rho \sin(\omega t + \phi) = \|G(j\omega)\| \sin(\omega t + \angle G(j\omega))$$

Summary 5. The steady-state response of a stable linear system with transfer function $G(s)$ to a sinusoidal input of the form $\sin(\omega t)$ is a sinusoid of the same frequency, but with amplitude $\|G(j\omega)\|$ and phase shift $\angle G(j\omega)$, i.e.

$$c_{\text{ss}}(t) = \|G(j\omega)\| \sin\left(\omega t + \angle G(j\omega)\right).$$

$\|G(j\omega)\|$ is also called the *gain*.

Example 17. Consider a system with transfer function $G(s) = \frac{s}{(s+1)(s+2)}$. We would like to compute the responses of this system to the following inputs

- $r_1(t) = \sin(3t)$;
- $r_2(t) = 2\sin(3t) + \cos(5t + 2)$.

To compute the response to r_1, we first calculate $G(3j)$ in polar form as: $G(3j) = \frac{3j}{(3j+1)(3j+2)} = 0.26e^{-0.66j}$. Thus, the steady-state response to $\sin(3t)$ is

$$c_{\text{ss1}}(t) = 0.26\sin(3t - 0.66).$$

Figure 3.1 shows the input r_1 and the output c_1. We can see that, after some transients, the output is a sinusoid with amplitude 0.26 and with a phase shift of -0.66 (or a phase lag of 0.66).

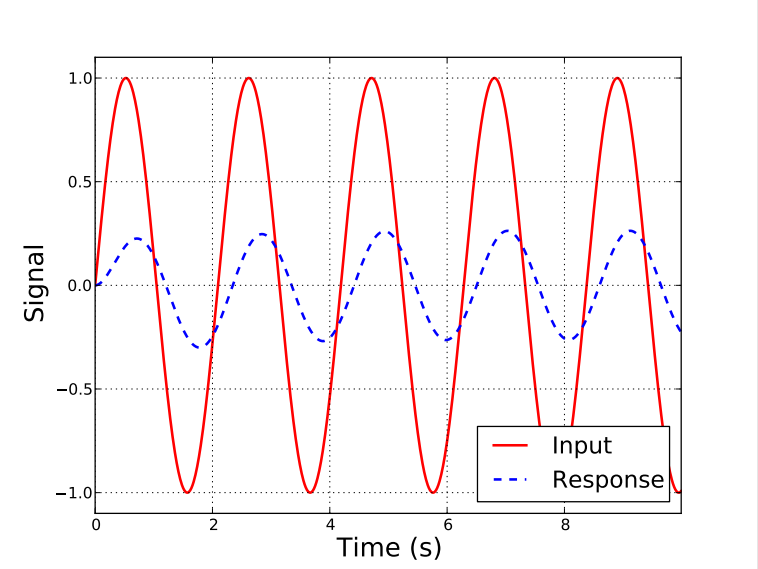

Figure 3.1: Response of system with transfer function $G(s) = \frac{s}{(s+1)(s+2)}$ to the input $r_1(t) = \sin(3t)$.

Next, to compute the response to r_2, we use the superposition principle.

- From above, the steady-state response to $2\sin(3t)$ is

$$2 * 0.26\sin(3t - 0.66) = 0.52\sin(3t - 0.66).$$

- We have $G(5j) = \frac{5j}{(5j+1)(5j+2)} = 0.18e^{-0.99}$. Thus, the steady-state response to $\cos(5t+2)$ is

$$0.18\cos(5t+2-0.99) = 0.18\cos(5t+1.01).$$

Finally, the steady-state response of the system to $r_2(t)$ is given by (see Fig. 3.2)

$$c_{ss2}(t) = 0.52\sin(3t-0.66) + 0.18\cos(5t+1.01).$$

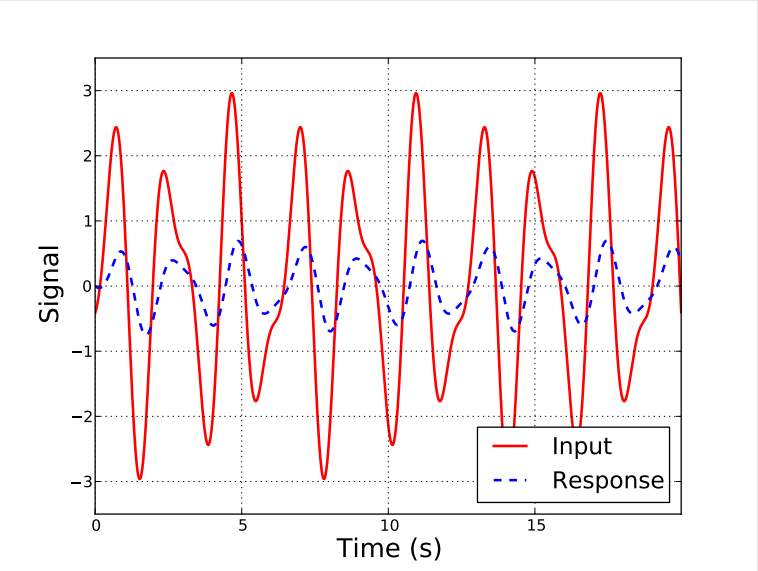

Figure 3.2: Response of system with transfer function $G(s) = \frac{s}{(s+1)(s+2)}$ to the input $r_2(t) = 2\sin(3t) + \cos(5t+2)$.

3.2 Bode plots : generalities

3.2.1 Interpretation of Bode plots

The previous section has shown that the response of a stable linear system with transfer function $G(j\omega)$ to a sinusoidal input of frequency ω is entirely determined by the amplitude and the phase of $G(j\omega)$. The Bode plots give a convenient representation of the amplitude and the phase of $G(j\omega)$ as a function of ω

- the amplitude plot shows $\|G(j\omega)\|$ as a function of ω. Since both ω and $\|G(j\omega)\|$ can have values in very large ranges, the plot is logarithmic: the scale of the X-axis – displaying the values of ω – is logarithmic;

the Y-axis displays $20\log(\|G(j\omega)\|)$. Note that log is taken in base 10 and that the unit of the Y-axis is the *decibel* (dB);

- the phase plot shows $\angle G(j\omega)$ as a function of ω. The scale of the X-axis – displaying the values of ω – is logarithmic; the Y-axis displays the phase shift in radian or degrees and in normal scale.

If we know the transfer function of the system, it is easy to sketch its Bode plots, as shown in Section 3.3. If we do *not* know the system TF, then the Bode plots can be constructed experimentally by subjecting the system to inputs of different frequencies and by reporting the amplitude and phase shift of the responses.

Conversely, from the Bode plots, it is very easy to compute the response of the system at a given frequency, as shown in Example 18. We can also obtain qualitative and quantitative insight into the system by analyzing the Bode plots, as shown in Section 3.4.

Example 18. Consider a system whose transfer function $G(s)$ is represented by the Bode plots in Fig. 3.3. We would like to determine graphically the steady-state response of this system to the following inputs

- $r_1(t) = \sin(0.01t)$;
- $r_2(t) = \cos(1000t + \pi/3)$.
- $r_3(t) = r_1(t) + r_2(t)$.

By reading on the Bode plots, we found that

- For $\omega = 0.01$, the gain is $\simeq -45\,\text{dB}$. We have $20\log(\|G(j\omega)\|) = -45$, thus $\|G(j\omega)\| = 10^{-45/20} = 0.0056$. Next, the phase shift is $\simeq \frac{\pi}{2}\,\text{rad}$. Thus, the steady-state response for r_1 is approximately

$$c_{\text{ss1}} \simeq 0.0056\sin(0.01t + \pi/2).$$

- For $\omega = 1000$, the gain is $\simeq 0\,\text{dB}$, which corresponds to ($\|G(j\omega)\| = 1$. The phase shift is $\simeq 0\,\text{rad}$. Thus the response to r_2 is approximately the same as r_2, i.e.

$$c_{\text{ss2}} \simeq r_2 = \cos(1000t + \pi/3).$$

By the superposition principle, the response to r_3 is the sum of the responses to r_1 and r_2. However, we can see that the response to r_1 is very small with respect to that of r_2, so it can be neglected. Thus

$$c_{\text{ss3}} \simeq c_{\text{ss2}} \simeq \cos(1000t + \pi/3).$$

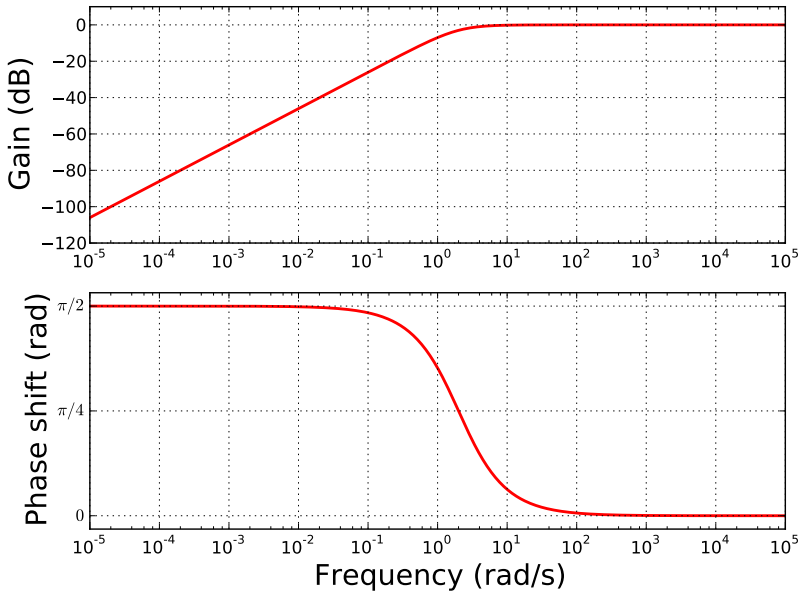

Figure 3.3: Bode plots of a system with unknown transfer function.

3.2.2 Filters

Bode plots are particularly suited to visualize the behaviors of filters. Consider for instance the circuit below

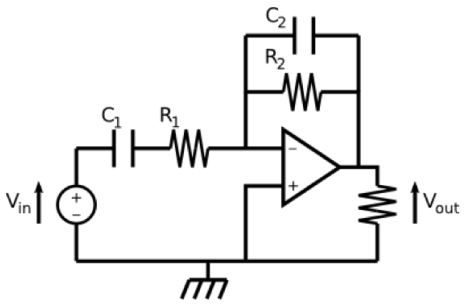

Figure 3.4: A circuit with an operational amplifier.

After some circuit calculations (see MA2009), the transfer function of this circuit can be determined as

$$G(j\omega) = \frac{V_{\text{out}}}{V_{\text{in}}} = -\frac{R_2}{R_1}\frac{j\frac{\omega}{\omega_1}}{\left(1+j\frac{\omega}{\omega_1}\right)\left(1+j\frac{\omega}{\omega_2}\right)},$$

where

$$\omega_1 = \frac{1}{R_1 C_1}, \quad \omega_2 = \frac{1}{R_2 C_2}.$$

The Bode plots of this circuit (with $R_1 = 1\Omega, R_2 = 10\Omega, C_1 = 1\text{mF}, C_2 = 1\mu\text{F}$) can then be obtained as below

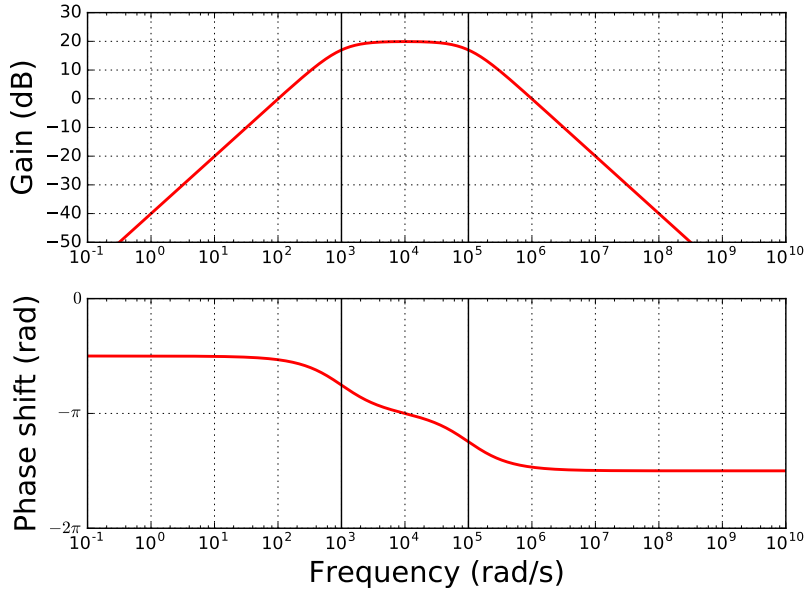

Figure 3.5: Bode plot of the circuit. The black vertical lines indicate the positions of $\omega_1 = 10^3$ and $\omega_2 = 10^5$.

One can observe, in the gain plot, that the gain is maximal for $\omega \in [\omega_1, \omega_2]$. Outside of that range, for $\omega \to 0$ and $\omega \to \infty$, the gain decreases quickly and converges to 0. Thus, one can say that the circuit is a *band-pass* filter, with the passband being $[\omega_1, \omega_2]$.

Low-pass and high-pass filters can be similarly conveniently visualized by their Bode plots.

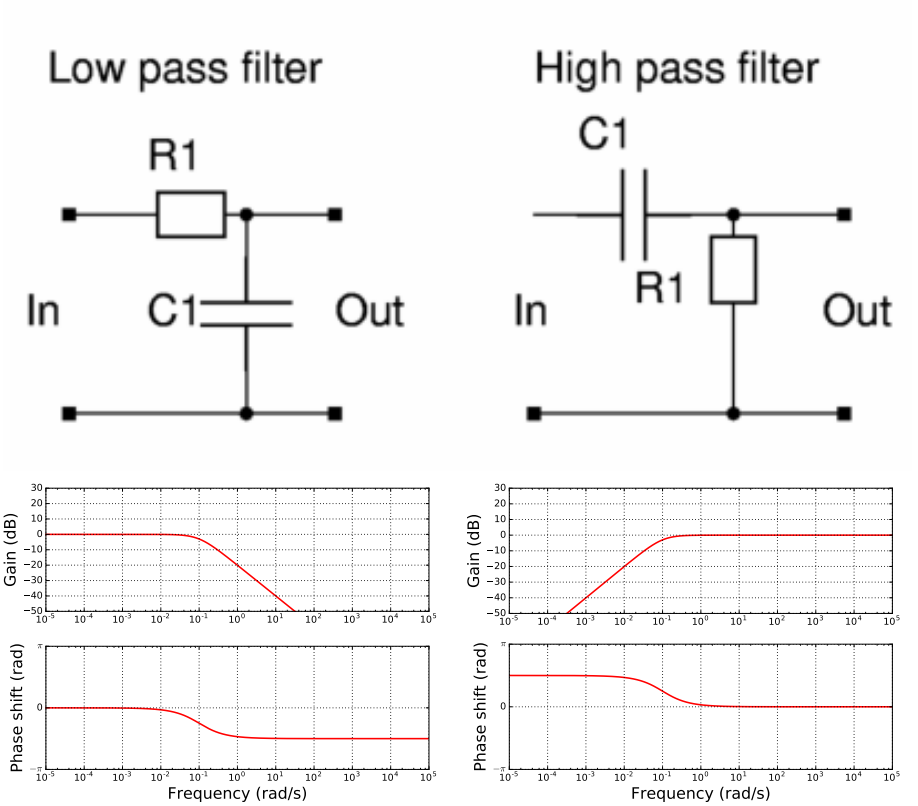

Figure 3.6: Low and high pass filters and their Bode plots. The cut-off frequency is $\omega = 0.1$ for both circuits.

3.3 Bode plots : sketching

3.3.1 Properties

Consider two systems with transfer functions $G(s)$ and $H(s)$. Remark that

$$20\log(\|G(j\omega)H(j\omega)\|) = 20\log(\|G(j\omega)\|) + 20\log(\|H(j\omega)\|),$$

$$\angle(G(j\omega)H(j\omega)) = \angle(G(j\omega)) + \angle(H(j\omega)).$$

Thus, the Bode plots of $G(s)H(s)$ can be obtained by *adding* those of $G(s)$ and $H(s)$. In practice, to sketch the Bode plots of a complex function, we can

- decompose the complex function into a product of basic functions;
- sketch the Bode plots of the basic functions;
- add the Bode plots of the basic functions to obtain those of the original function.

Another interesting point to remark is that

$$20\log\left(\left\|\frac{1}{G(j\omega)}\right\|\right) = -20\log(\|G(j\omega)\|),$$

$$\angle\left(\frac{1}{G(j\omega)}\right) = -\angle(G(j\omega)).$$

Thus, the Bode plots of $1/G(s)$ can be obtained by flipping that of $G(s)$ with respect to the X-axis.

3.3.2 Bode plots of basic functions

In this section, we shall designate by y the coordinate of the Y-axis and x the log-coordinate of the X-axis, i.e. $x = \log(\omega)$. Thus, a straight line in the Bode plot of the amplitude will have equation $y = ax + b$.

Constant terms

For a constant real positive gain K, $20\log(|K|)$ is a constant independent of ω, so the amplitude plot is a horizontal line with $y = 20\log(|K|)$. Note that

- $y > 0$ if $K > 1$;
- $y = 0$ if $K = 1$;
- $y < 0$ if $K < 1$.

Next, $\angle K = 0$, thus the phase plot is a horizontal line with $y = 0$. Fig. 3.7 shows the Bode plots for two values of K.

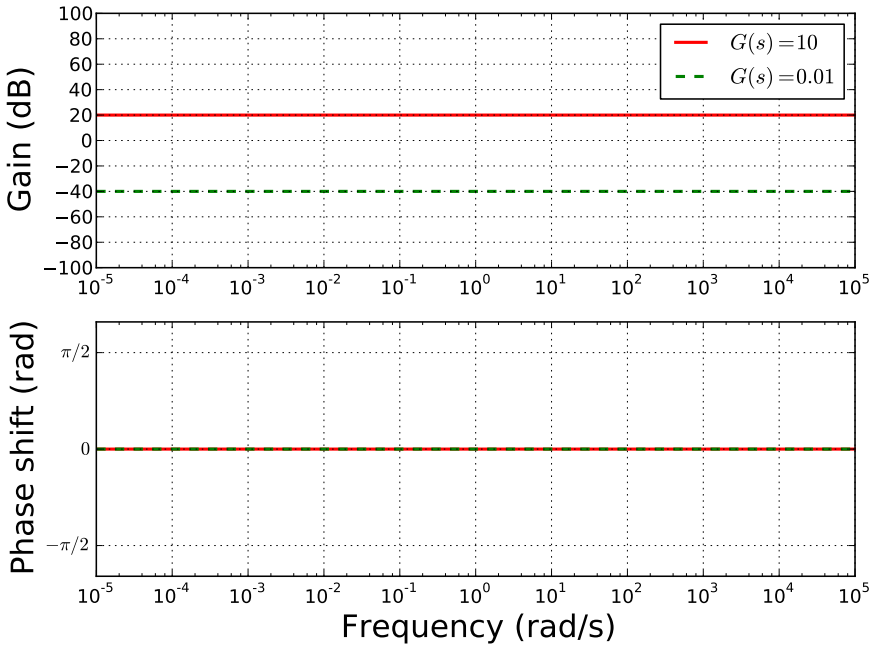

Figure 3.7: Bode plots for constant gains.

Derivative and integral terms

Consider the derivative term $G(s) = s$.

- We have $20\log(\|G(j\omega)\|) = 20\log(\|j\omega\|) = 20\log(\omega)$. Thus the Bode plot of the gain is a straight line with slope $+20$: every decade, the line goes up 20 dB. For $\omega = 1$, we have $20\log(\omega) = 0$, so the line goes through the point $(x, y) = (0, 0)$;
- We have $\angle G(j\omega) = \angle j = \pi/2$. Thus the Bode plot of the phase is a horizontal line with $y = \pi/2$.

The Bode plots of the integral term $G(s) = 1/s$ are the symmetric of those of the derivative terms with respect to $y = 0$. In particular

- The gain plot is a straight line with slope -20;
- The phase plot is a horizontal line with $y = -\pi/2$.

Fig. 3.8 shows the Bode plots of the derivative and integral terms.

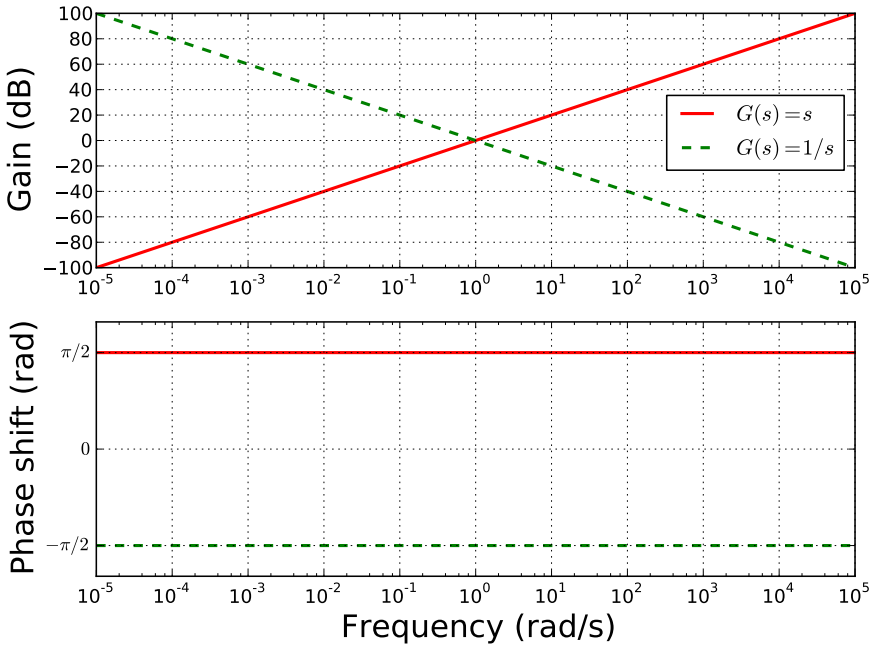

Figure 3.8: Bode plots for derivative and integral terms.

First-order terms

Consider the transfer function $G(s) = s + a$. Regarding the gain plot,

- when $\omega \to 0$, $20\log(\|j\omega + a\|) \simeq 20\log(a)$. Thus the asymptote to the left is a horizontal line with $y = 20\log(a)$;
- when $\omega \to \infty$, $20\log(\|j\omega + a\|) \simeq 20\log(\|j\omega\|) = 20\log(\omega)$. Thus, the asymptote to the right is a straight line with slope +20 (equation $y = 20x$);
- the two asymptotes meet when $20\log(a) = 20x$, i.e. $\log(a) = x = \log(\omega)$, i.e. $\omega = a$. This intersection frequency $\omega = a$ is called the *corner frequency*.

Regarding the phase plot

- when $\omega \to 0$, $\angle(j\omega + a) \simeq \angle a = 0$. Thus the asymptote to the left is a horizontal line with $y = 0$;
- when $\omega \to \infty$, $\angle(j\omega + a) \simeq \angle j\omega = \pi/2$. Thus, the asymptote to the right is a horizontal line with $y = \pi/2$;
- the transition occurs around the corner frequency $\omega = a$.

The Bode plots of $G(s) = 1/(s + a)$ are the symmetric of those of the derivative terms with respect to $y = 0$. In particular

- the gain plot follows a horizontal asymptote $y = -\log(a)$ on the left, and a inclined asymptote with slope -20 on the right. The two asymptotes meet at the corner frequency $\omega = a$;
- the phase plot follows a horizontal asymptote $y = 0$ on the left, and a horizontal asymptote $y = -\pi/2$ on the right. The transition occurs around the corner frequency $\omega = a$.

Fig. 3.9 shows the Bode plots for $G(s) = s + a$ and $G(s) = 1/(s + a)$ with $a = 0.1$.

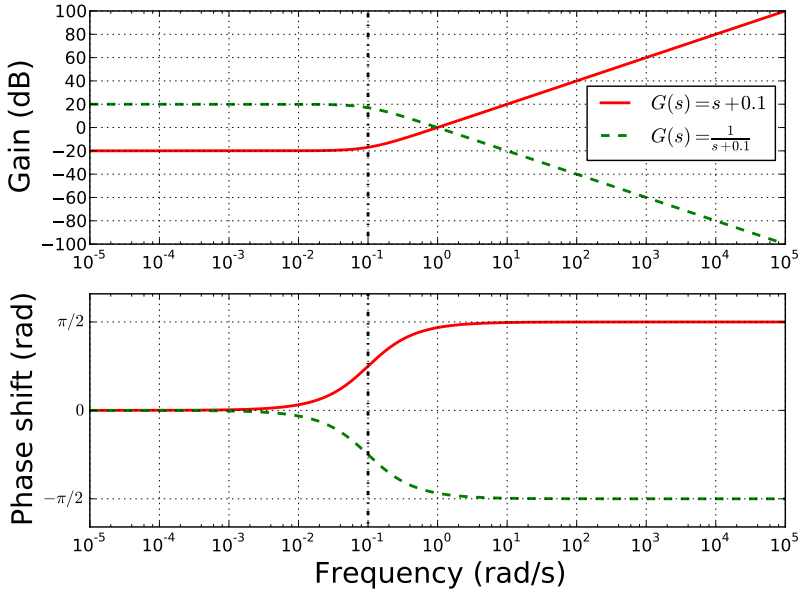

Figure 3.9: Bode plots for first-order terms $G(s) = s+a$ and $G(s) = 1/(s+a)$ with $a = 0.1$. The corner frequency $\omega = a$ is indicated by a vertical dashed-dotted black line.

Second-order terms

Typical second-order terms we shall encounter have the following form

$$G(s) = \frac{\omega_n^2}{s^2 + 2\zeta\omega_n s + \omega_n^2}.$$

Note that changing the term ω_n^2 in the numerator to another constant does not change the shape of the curve but will only shift the curve up or

down. However, it is important to scale the second-order term $s^2+2\zeta\omega_n s+\omega_n^2$ so that the leading coefficient is 1.

After dividing the numerator and the denominator by ω_n^2, we have

$$G(j\omega) = \frac{1}{1 - \frac{\omega^2}{\omega_n^2} + 2j\zeta\frac{\omega}{\omega_n}}.$$

Note that

- when $\omega \to 0$, we have $\frac{\omega}{\omega_n} \to 0$, thus, $G(j\omega) \to 1$;
- when $\omega \to \infty$, 1 and $2j\zeta\frac{\omega}{\omega_n}$ are negligible compared to $\frac{\omega^2}{\omega_n^2}$, thus $G(j\omega) \simeq -\frac{\omega_n^2}{\omega^2}$.

The above analysis leads to the following observations regarding the gain plot

- the asymptote on the left is a horizontal line with $y = 0$;
- on the right, we have

  $$20\log(\|G(j\omega\|) \simeq 20\log(\omega_n^2/\omega^2) = 40(\log(\omega_n) - \log(\omega)).$$

  Thus, the asymptote is a line with equation $y = 40\log(\omega_n) - x$.
- The two asymptotes meet when $0 = 40\log(\omega_n) - x$, i.e. when $\omega = \omega_n$. Thus ω_n is the corner frequency.

Regarding the phase plot,

- the asymptote on the left is a horizontal line with $y = 0$;
- the asymptote on the right is a horizontal line with $y = -\pi$;
- the transition occurs around the corner frequency $\omega = \omega_n$.

Fig. 3.10 shows the Bode plots of second-order terms for different values of ζ. Note that, while ζ has no influence on the asymptotes, it affects the transition around the corner frequency

- low values of ζ ($\zeta < 0.707$) yield a peak in the gain plot (the smaller ζ, the higher the peak) and a sharp decrease in the phase plot around the corner frequency;
- high values of ζ ($\zeta > 0.707$) yield a monotonically decreasing gain and a slow decrease in the phase plot around the corner frequency.

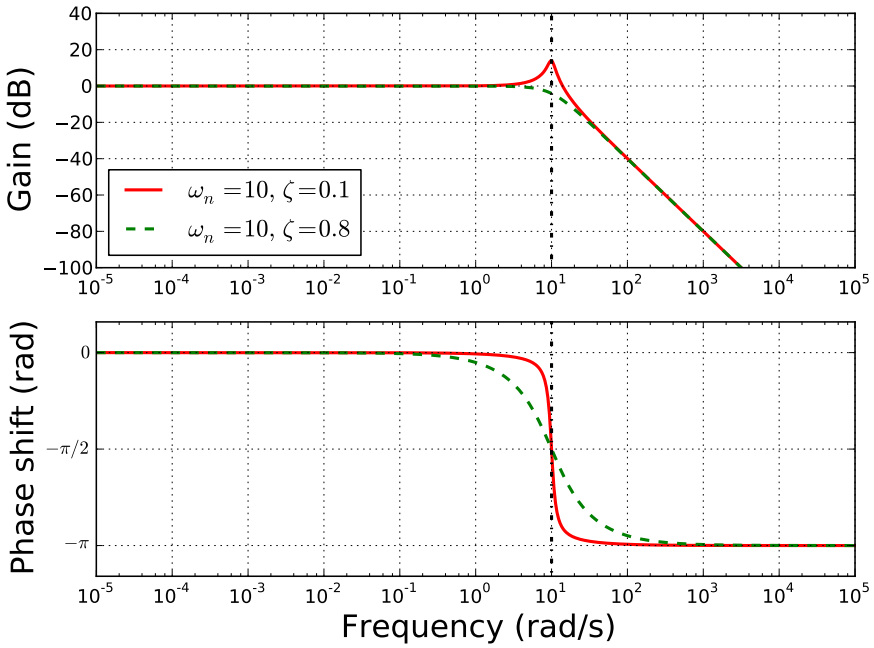

Figure 3.10: Bode plots for second-order terms for $\omega_n = 10$ (indicated by a vertical dashed-dotted black line) and for different values of ζ.

3.3.3 Bode plots of complex functions

As mentioned previously, one may sketch the Bode plots complex function by

- decomposing the complex function into a product of basic functions;
- sketching the Bode plots of the basic functions;
- adding the Bode plots of the basic functions to obtain those of the original function.

However, the above approach can be tedious. Here we present another approach, which is simpler but which requires more function evaluations. In this approach, a Bode plot (gain or phase) is composed of three parts:

1. Left part : from $\omega \simeq 0$ to $\omega = 0.1\omega_{\text{min}}$ where ω_{min} is the smallest corner frequency. In this part, the plots will be represented by their left asymptotes;
2. Middle part : from $\omega = 0.1\omega_{\text{min}}$ to $\omega = 10\omega_{\text{max}}$ where ω_{max} is the largest corner frequency. In this part, the plots will be constructed by sampling and numerical evaluations;

3. Right part : from $\omega = 10\omega_{\max}$ to $\omega \simeq \infty$. In this part, the plots will be represented by their right asymptotes.

Left asymptotes

Assume that the system is of type k, i.e.

$$G(s) = \frac{N(s)}{s^k D(s)},$$

with $N(0) \neq 0$ and $D(0) \neq 0$. Note that we are interested in the function G itself, not the corresponding unity-feedback function $G/(1+G)$.

Regarding the gain plot, we have, when $\omega \to 0$

$$20\log(\|G(j\omega)\|) \simeq 20\log\left(\frac{|N(0)|}{\omega^k |D(0)|}\right) = 20\log\left(\frac{|N(0)|}{|D(0)|}\right) - 20k\log(\omega).$$

Thus, the asymptote on the left will be straight line with slope $-20k$ dB/decade. To find one point on this line, we may evaluate the equation of the line at e.g. $\omega = 1$, to find that the line must pass through $(x, y) = (0, 20\log(|N(0)/D(0)|)$. Note that the asymptote might stop before $\omega = 1$ in case $\omega_{\min} < 1$.

Regarding the angle plot, we have, when $\omega \to 0$

$$\angle G(j\omega) \simeq \angle(N(0)/D(0)) - k\angle(j\omega).$$

Thus,

- if $N(0)/D(0) > 0$, we have a horizontal asymptote with $y = -k\pi/2 \mod 2\pi$;
- if $N(0)/D(0) < 0$, we have a horizontal asymptote with $y = \pi - k\pi/2 \mod 2\pi$.

Right asymptotes

Assume that the system is of order n, i.e.

$$G(s) = \frac{N(s)}{D(s)},$$

with $\deg(D) - \deg(N) = n$. Note that we are interested in the function G itself, not the corresponding unity-feedback function $G/(1+G)$.

Regarding the gain plot, we have, when $\omega \to \infty$

$$20\log(\|G(j\omega)\|) \simeq 20\log\left(\frac{|A|}{\omega^n}\right) = 20\log|A| - 20n\log(\omega),$$

where A is the ratio of the leading coefficient of N to the leading coefficient of D. Thus, the asymptote on the right will be straight line with

slope $-20n$ dB/decade. To find one point on this line, we may evaluate the equation of the line at e.g. $\omega = 1$, to find that the line must pass through $(x, y) = (0, 20 \log |A|)$. Note that the asymptote might stop before $\omega = 1$ in case $\omega_{\max} > 1$.

Regarding the angle plot, we have, when $\omega \to \infty$

$$\angle G(j\omega) \simeq \angle A - n\angle(j\omega).$$

Thus,

- if $A > 0$, we have a horizontal asymptote with $y = -n\pi/2 \mod 2\pi$;
- if $A < 0$, we have a horizontal asymptote with $y = \pi - n\pi/2 \mod 2\pi$.

Middle part

The middle part ranges from $\omega = 0.1\omega_{\min}$ to $\omega = 10\omega_{\max}$. Here, we simply *sample* some points in the interval $(0.1\omega_{\min}, 10\omega_{\max})$ and evaluate *numerically* $20 \log(\|G(j\omega)\|)$ and $\angle G(j\omega)$. Since the plots tend to display large variations around the corner frequencies, we shall sample more densely around the corner frequencies.

Example 19. Let us sketch the Bode plots of the transfer function

$$G(s) = \frac{-5(s + 0.1)}{s^2(s^2 + 0.1s + 49)}$$

Step 1 Identify the corner frequencies:

- the first-order term $s+0.1$ has a corner frequency at $\omega = 0.1$;
- the second-order term $s^2 + 0.1s + 49$ has a corner frequency at $\omega = \sqrt{49} = 7$.

Thus, $\omega_{\min} = 0.1$ and $\omega_{\max} = 7$.

Step 2 Left part. We have a term $1/s^2$, thus system type is 2. The gain plot therefore has a left asymptote with slope -40 dB/decade and going through the point

$$(x, y) = \left(0, 20 \log \left(\frac{0.5}{49}\right)\right) = (0, -39.82).$$

The phase plot has a horizontal left asymptote with

$$y = \pi - 2 * \frac{\pi}{2} = 0.$$

Step 3 Right part. The numerator has degree 1 and the denominator has degree 4, thus the system order is $4 - 1 = 3$. The gain plot

therefore has a right asymptote with slope $-60\,\mathrm{dB}$/decade. The leading coefficient of the numerator is -5, the leading coefficient of the denominator is 1, thus $A = -5$. The right asymptote thus goes through the point

$$(x, y) = (0, 20 \log 5) = (0, 13.98).$$

The phase plot has a horizontal right asymptote with

$$y = \pi - 3 * \frac{\pi}{2} = -\frac{\pi}{2}.$$

Step 4 Middle part. We sample the X-axis for $\omega \in (0.01, 70) = (10^{-2}, 10^{1.85})$.

x	ω	$20 \log(\|G(j\omega)\|)$	$\angle G(j\omega)$
-2	0.01	40.22	0.1
-1.5	0.03	20.59	0.31
-1	0.1	3.19	0.79
-0.5	0.32	-9.39	1.26
0	1.0	-19.6	1.47
0.5	3.16	-27.84	1.53
1	10.0	-40.17	-1.56
1.5	31.62	-75.58	-1.57
1.85	70.79	-96.94	-1.57

Now, we sample more densely around $\omega = 0.1$ and $\omega = 7$.

x	ω	$20 \log(\|G(j\omega)\|)$	$\angle G(j\omega)$
-1.15	0.07	7.94	0.62
-1.1	0.08	6.3	0.67
-1.05	0.09	4.72	0.73
-1	0.1	3.19	0.79
-0.95	0.11	1.72	0.84
-0.9	0.13	0.3	0.9
-0.85	0.14	-1.06	0.95

x	ω	$20 \log(\|G(j\omega)\|)$	$\angle G(j\omega)$
0.7	5.01	-27.58	1.53
0.75	5.62	-25.82	1.52
0.8	6.31	-21.31	1.49
0.85	7.08	-5.46	-1.02
0.9	7.94	-27.02	-1.53
0.95	8.91	-34.69	-1.55
1	10.0	-40.17	-1.56

Step 5 We can now sketch the Bode plots in Fig. 3.11. For $\omega < 0.01$, we use the left asymptotes (both gain and phase plots). For $\omega \in (0.01, 70)$, we use the sampled points joined by straight segments. For $\omega > 70$, we use the right asymptotes.

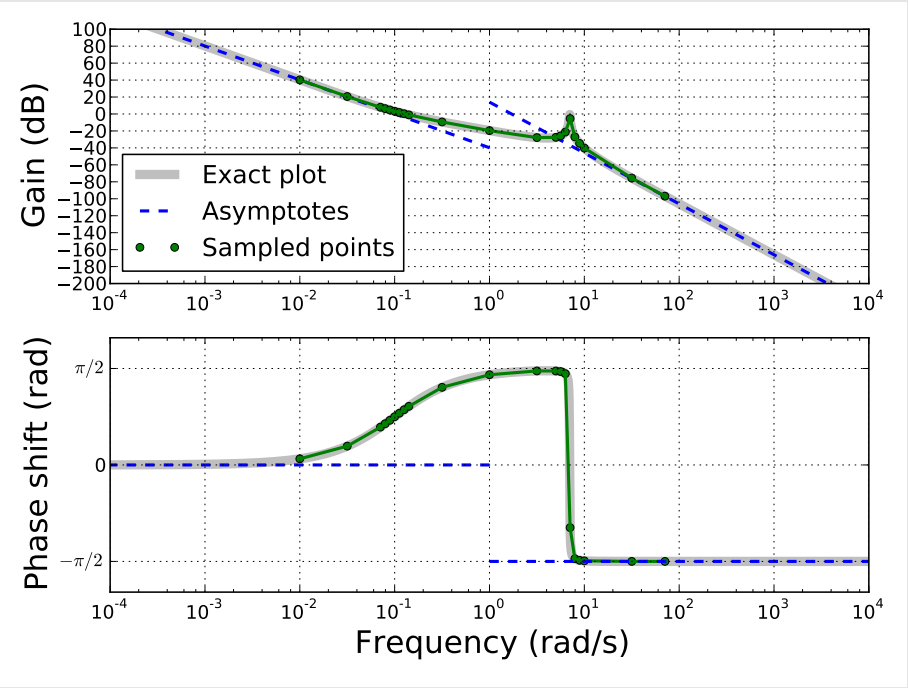

Figure 3.11: Bode plots for a complex function. The exact Bode plots are in bold light gray. The asymptotes are in dashed blue. The sampled points are green and joined by green segments. We can see that the plots sketched by the method presented previously approximate quite well the exact Bode plots.

3.4 Bode plots : analysis

Assume now that we are given a system but that we do not know its transfer function. We can subject the system to sinusoidal inputs of various frequencies and report the amplitude of the system responses. Doing so will enable us to *experimentally* sketch the Bode plot of the gain of the system.

Next, from this experimental Bode plot, we can reverse-engineer some important information about the system itself.

3.4.1 Determining system type and system order

In Section 3.3.3, we found that a system of type k has a left asymptote with slope $-20k\,\text{dB/decade}$. Thus, from the experimental the Bode plot of the gain, we can

- fit a straight line to the *extreme left* portion of the plot;
- compute the slope σ_{left} of this line;
- obtain the system type by rounding $-\sigma_{\text{left}}/20$ to the closest integer.

Similarly, regarding the system order, we can

- fit a straight line to the *extreme right* portion of the gain plot;
- compute the slope σ_{right} of this line;
- obtain the system type by rounding $-\sigma_{\text{right}}/20$ to the closest integer.

3.4.2 Determining position and velocity constants and steady-state errors

Type-0 systems

Assume that we have determined that a given system is of type 0, (in other words, we have found that the gain plot has a horizontal left asymptote). If the transfer function of the system is G, then the Y-coordinate of this asymptote is given by

$$\lim_{\omega\to 0} 20\log(\|G(j\omega)\|) = 20\log(|G(0)|) = 20\log K_p,$$

where K_p is the position constant. Thus, we can find the position constant of a type-0 system as follows

- denote by $y_{\text{asymptote}}$ the Y-coordinate of the horizontal left asymptote;
- compute K_p by $K_p = 10^{\frac{y_{\text{asymptote}}}{20}}$.

Finally, we can also compute the steady-state error to step input of the corresponding unity-feedback system (whose TF is $G/(1+G)$) by

$$e_{ss} = \frac{1}{1+K_p}.$$

Example 20. We have experimentally determined the gain plot of a system with unknown transfer function in Fig. 3.12.

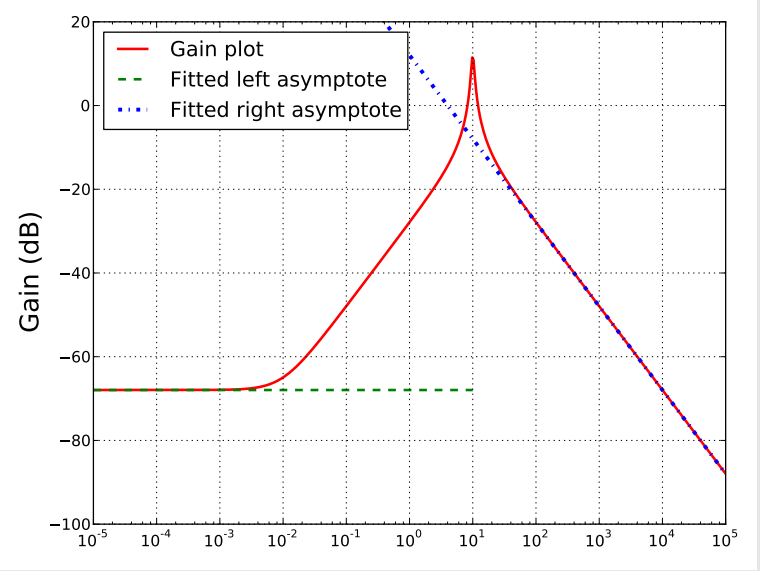

Figure 3.12: Gain plot of a system with unknown transfer function. Straight lines (green dashed and blue dashed-dotted) are fitted to the extreme left and right portions of the plot.

The left asymptote is horizontal, indicating a system type $k = 0$. The right asymptote has a slope of $-20\,\text{dB/decade}$, indicating a system order $n = 1$.

Next, since the system is of type 0, we can calculate the position constant K_p. We determine graphically that the Y-coordinate of the horizontal asymptote is $y_{\text{asymptote}} \simeq -68\,\text{dB}$. Thus, the position constant is given by

$$K_p \simeq 10^{-68/20} \simeq 0.0004.$$

Finally, the steady-state error to unit step input of the corresponding unity-feedback system is

$$e_{ss} = \frac{1}{1 + K_p} \simeq 1.$$

Type-1 systems

Assume that we have determined that a given system is of type 1, (in other words, we have found that the gain plot has a left asymptote with slope $-20\,\text{dB/decade}$). Thus, the transfer function of the system has the form

$$G(s) = \frac{N(s)}{sD(s)},$$

with $N(0) \neq 0$ and $D(0) \neq 0$. Next, the velocity constant of the system is given by

$$K_v = \frac{|N(0)|}{|D(0)|}.$$

On the other hand, we noted in Section 3.3.3 that the left asymptote goes through the point $(x, y) = (0, 20\log(|N(0)/D(0)|)$. Thus, we can find the velocity constant of a type-1 system as follows

- determine the intersection of the left asymptote with the vertical line $x = 0$ (or $\omega = 1$) and denote by $y_{\text{intersect}}$ the Y-coordinate of this intersection;
- compute K_v by $K_v = 10^{\frac{y_{\text{intersect}}}{20}}$.

Finally, we can also compute the steady-state error to ramp input of the corresponding unity-feedback system (whose TF is $G/(1+G)$) by

$$e_{ss} = \frac{1}{K_v}.$$

Example 21. We have experimentally determined the gain plot of a system with unknown transfer function in Fig. 3.13.

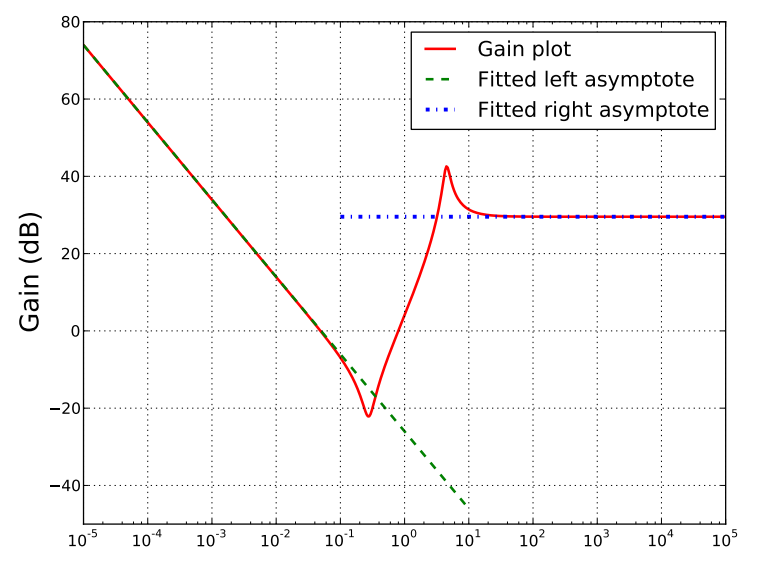

Figure 3.13: Gain plot of a system with unknown transfer function. Straight lines (green dashed and blue dashed-dotted) are fitted to the extreme left and right portions of the plot.

The left asymptote has a slope of $-20\,\text{dB/decade}$, indicating a system type $k = 1$. The right asymptote is horizontal, indicating a system

order $n = 0$.

Next, since the system is of type 1, we can calculate the velocity constant K_v. We determine graphically that the left asymptote intersects the vertical line $x = 0$ (or $\omega = 1$) at a point with Y-coordinate $y_{\text{intersect}} \simeq -26\,\text{dB}$. Thus, the velocity constant is given by

$$K_v \simeq 10^{-26/20} \simeq 0.05.$$

Finally, the steady-state error to unit ramp input of the corresponding unity-feedback system is

$$e_{ss} = \frac{1}{K_v} \simeq 20.$$

3.4.3 Stability margins

Nyquist stability criterion

In the the previous section, we showed that the Bode plots of an open-loop system can give information about the *steady-state errors* of the corresponding unity-feedback system. Here, we show how the open-loop Bode plots can also tell us whether the corresponding unity-feedback system is *stable*. This is done through the following theorem

Theorem 1 (Nyquist stability criterion)**.** Consider a stable system with transfer function G. The corresponding unity-feedback system (whose transfer function is $G/(1+G)$) is stable if and only if

$$\|G(j\omega)\| < 1 \quad \text{when} \quad \angle G(j\omega) = \pm\pi \mod 2\pi. \tag{3.2}$$

An equivalent condition is

$$\angle G(j\omega) > -\pi \quad \text{when} \quad \|G(j\omega)\| = 1. \tag{3.3}$$

Example 22. Consider a system with transfer function

$$G = \frac{200}{(s+2)(s+4)(s+5)}.$$

The Bode plots of this system is presented in Fig. 3.14, red plain lines.

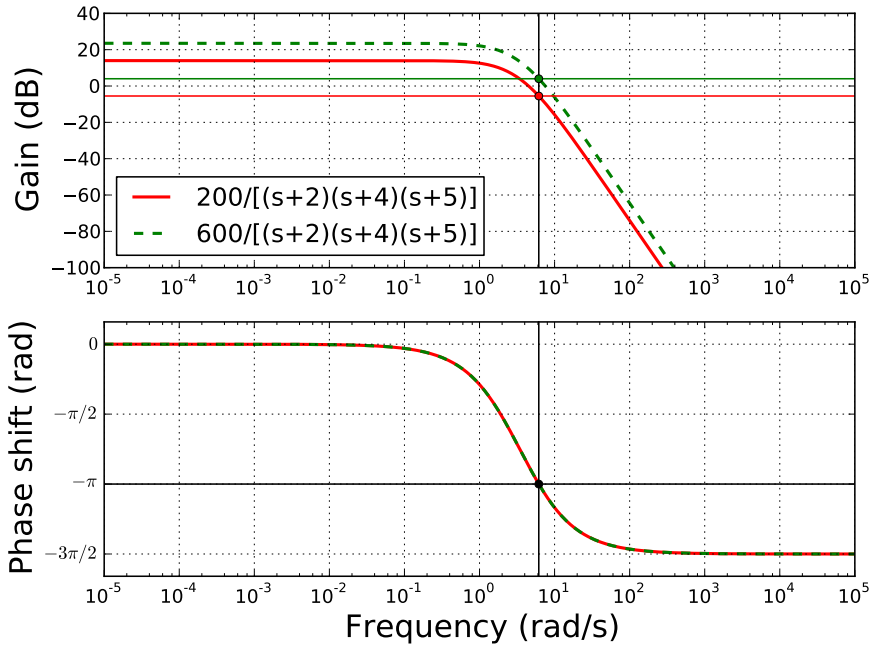

Figure 3.14: Nyquist criterion (gain condition).

Let us determine whether the corresponding unity-feedback system is stable using the (first) Nyquist criterion 3.2. From the phase plot, we can see that $\angle G(j\omega) = -\pi$ for $\omega \simeq 6.6\,\text{rad/s}$. Consider now the gain plot. At $\omega = 6.6\,\text{rad/s}$, we find that the gain in dB is *negative* (around -5.5 dB), which means that $\|G(j\omega)\| < 1$. Therefore, we can conclude that the corresponding unity-feedback system is *stable*.

Consider a system with transfer function

$$G_2 = \frac{600}{(s+2)(s+4)(s+5)}.$$

The Bode plots of this system is presented in Fig. 3.14, green dashed lines. From the phase plot, we can see that $\angle G_2(j\omega) = -\pi$ for $\omega \simeq 6.6\,\text{rad/s}$ (same as for the previous system, since the constant gains – 600 or 200 – do not contribute to the phase). In the gain plot, we find that the gain in dB at $\omega \simeq 6.6$ is *positive* (around +4 dB), which means that $\|G_2(j\omega)\| > 1$. Therefore, we can conclude that the corresponding unity-feedback system is *unstable*.

Example 23. Consider again the system with transfer function

$$G = \frac{200}{(s+2)(s+4)(s+5)}.$$

The Bode plots of this system is presented in Fig. 3.14, red plain lines.

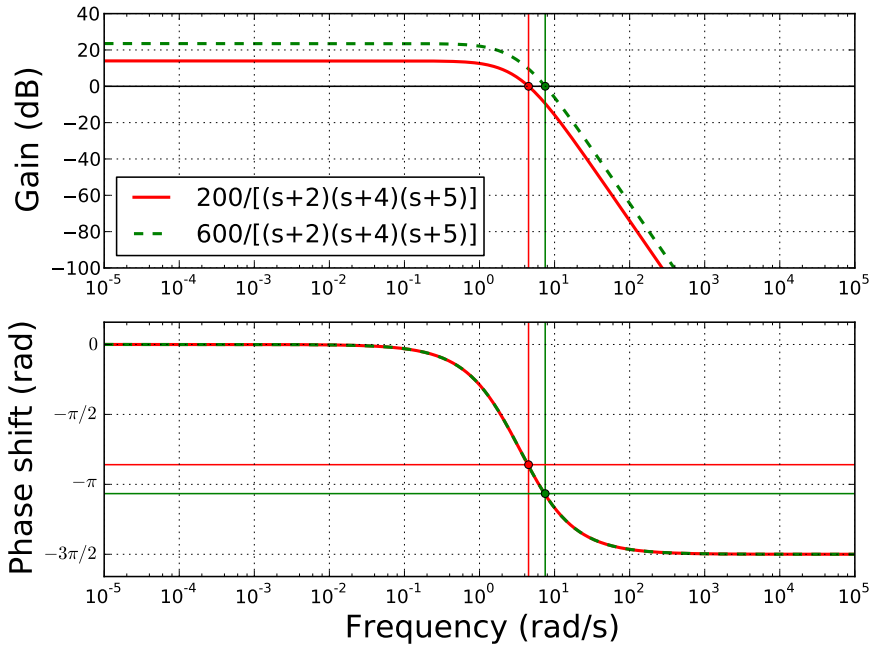

Figure 3.15: Nyquist criterion (phase condition).

Let us determine whether the corresponding unity-feedback system is stable using the (second) Nyquist criterion 3.2. From the phase plot, we can see that $\|G(j\omega)\| = 1$ for $\omega \simeq 4.5\,\text{rad/s}$. Consider now the phase plot. At $\omega = 4.5\,\text{rad/s}$, we find that the phase is $\angle G(j\omega) \simeq -2.7 > -\pi$. Therefore, we can conclude that the corresponding unity-feedback system is *stable*.

Consider the system with transfer function

$$G_2 = \frac{600}{(s+2)(s+4)(s+5)}.$$

The Bode plots of this system is presented in Fig. 3.14, green dashed lines. From the phase plot, we can see that the $\|G_2(j\omega_2)\| = 1$ for $\omega_2 \simeq 7.5\,\text{rad/s}$. In the phase plot, we find that $\angle G_2(j\omega_2) \simeq -3.35 <$

$-\pi$. Therefore, we can conclude that the corresponding unity-feedback system is *unstable*.

Gain margin and phase margin

We have seen in Example 22 that increasing the gain of the open-loop TF from 200 to 600 made the corresponding unity-feedback system become unstable. Can we determine from the Bode plots the *maximum* gain increase before the corresponding unity-feedback system becomes unstable ?

The answer is yes. Consider again the TF

$$G = \frac{200}{(s+2)(s+4)(s+5)}.$$

We saw that the frequency for which $\angle G(j\omega) = -\pi$ was $\omega \simeq 6.6\,\text{rad/s}$. Next, the gain at this frequency was found to be $20\log\|G(j\omega)\| = -5.5\,\text{dB}$.

Assume now that the TF has been multiplied by a factor K, so that the new TF is

$$KG = \frac{200K}{(s+2)(s+4)(s+5)}.$$

We have $\angle KG = \angle G$, so $\angle KG(j\omega) = -\pi$ also for $\omega \simeq 6.6\,\text{rad/s}$. Next, the gain at this frequency will be

$$20\log\|KG(j\omega)\| = 20\log K + 20\log\|G(j\omega)\| = 20\log K - 5.5\,\text{dB}.$$

If we want the unity-feedback system associated with KG to be stable, we must have, by the Nyquist criterion

$$20\log\|KG(j\omega)\| < 0,$$

which implies that $20\log K < 5.5\,\text{dB}$ (or $K < 10^{5.5/20} = 1.88$).

The value $G_M = 5.5\,dB$ is called the *gain margin* of system G: if we multiply G by a factor K such that $20\log K < G_M$, then the corresponing unity-feedback system remains stable ; if we multiply G by a factor K such that $20\log K > G_M$, then the corresponing unity-feedback system will become unstable.

To verify the latter assertion, consider again the transfer function $G_2 = \frac{600}{(s+2)(s+4)(s+5)}$. Remark that $G_2 = 3G$. Next, $20\log 3 = 9.54 > 5.5$. Thus, G has been increased by a factor larger than the gain margin, which implies that the unity-feedback system corresponding to G_2 will be unstable. This is confirmed by Example 22.

In general, we can see from the above development that the gain margin is given by $G_M = -20\log\|G(j\omega^*)\|$ where ω^* is the frequency that verifies $\angle G(j\omega^*) = -\pi$. Fig. 3.16 illustrates the evaluation of G_M for $G = \frac{200}{(s+2)(s+4)(s+5)}$.

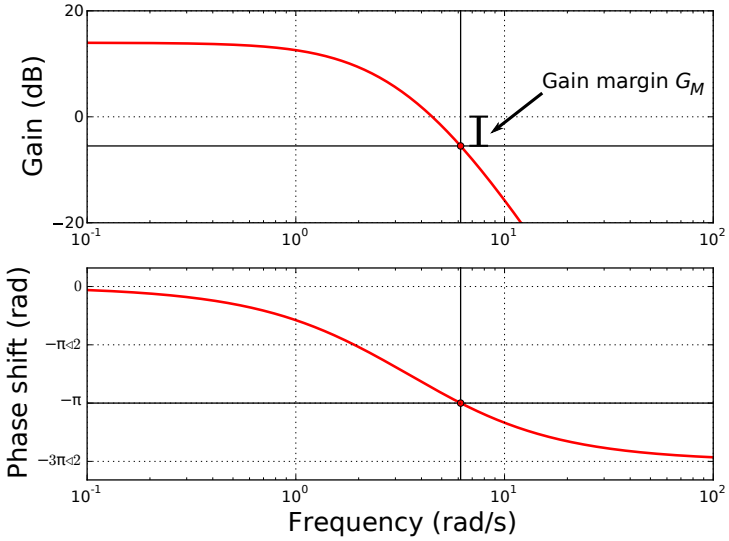

Figure 3.16: Gain margin for $G = \frac{200}{(s+2)(s+4)(s+5)}$.

Similarly, one can define the *phase margin* ϕ_M as follows: ϕ_M is the maximum angle that we can subtract to the open-loop transfer function before the corresponding unity-feedback feedback system becomes unstable. Formally, ϕ_M is given by $\phi_M = \pi + \angle G(j\omega^*)$ where ω^* is the frequency that verifies $\|G(j\omega^*)\| = 1$. For $G = \frac{200}{(s+2)(s+4)(s+5)}$, Example 23 showed that $\phi_M \simeq \pi - 2.7 \simeq 0.44\,\text{rad}$. Fig. 3.17 illustrates this evaluation.

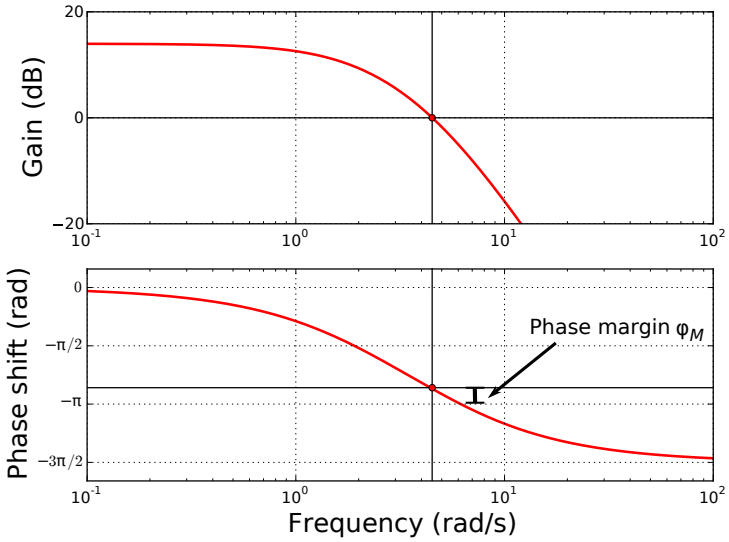

Figure 3.17: Phase margin for $G = \frac{200}{(s+2)(s+4)(s+5)}$.

Large stability margins (both gain and phase margins) ensure that the corresponding unity-feedback will be stable even if there are some variations in the system components. One can also say, roughly, that the larger the margins, the larger the damping (hence the more stable the unity-feedback system). Usually, a gain margin of at least 6 dB and a phase margin of 30 to 60 degrees are required ($\simeq 0.5$ to 1 rad).

3.4.4 Some remarks on controller design by the frequency-response method

Section 3.4.2 and 3.4.3 have shown us how the Bode plots of a system with transfer function G can give us information about the corresponding unity-feedback system (whose transfer function is $G/(1+G)$):

- Section 3.4.2 showed that the asymptotic behavior of G when $\omega \to 0$ can give information about the steady-state error to step inputs (type 0 system) or to ramp inputs (type 1 systems) of the corresponding unity-feedback system;
- Section 3.4.3 showed how to compute stability margins from the Bode plots of G, which give us information about the stability of the corresponding unity-feedback system.

In turn, this information can be used in controller design. Consider for instance the system of Example 21. We determined that its velocity constant was $K_v = 0.05$, which yields a steady-state error of the corresponding unity-feedback system to unit ramp input of $e_{ss} = 20$. If we want to decrease the steady-state error to one-tenth of this value (without considering the change in the transient behavior), we can for instance use a gain adjustment method whereby we would multiply the open-loop TF by a factor 10, which would result in $K_v^{\text{new}} = 0.5$, and $e_{ss}^{\text{new}} = 1/K_v^{\text{new}} = 2$.

The stability margins can be used in compensator design. Basically, we have seen in Section 2.4.2 that a lead compensator "added phase" to the system. Thus, one can improve the stability of a system (i.e. achieving larger phase margin) by adding a lead compensator that contribute the appropriate amount of phase. However, in practice, the design of lead/lag compensators is relatively involved, so it will not be covered here.